ZIRAT22 Annual Report

Authors

Charles Patterson
Clovis, CA, USA

Tahir Mahmood
Pleasanton, CA, USA

Kit Coleman
Deep River, ON, Canada

Albert Machiels
Brentwood, CA, USA

Ronald Adamson
Fremont, CA, USA

A.N.T. INTERNATIONAL®

Ecolabelled printed matter, 4041 0799

Disclaimer

The information presented in this report has been compiled and analysed by
Advanced Nuclear Technology International Europe AB (ANT International®) and its subcontractors.
ANT International has exercised due diligence in this work, but does not warrant the accuracy or
completeness of the information. ANT International does not assume any responsibility for any
consequences as a result of the use of the information for any party, except a warranty
for reasonable technical skill, which is limited to the amount paid for this report.

Quality-checked and authorized by:

Mr Peter Rudling, President of ANT International

Contents

1 Introduction

The objective of the Annual Review of ZIRconium Alloy Technology (ZIRAT) and Information on Zirconium Alloys (IZNA) is to review and evaluate the latest developments in ZIRAT as they apply to nuclear fuel design and performance.

The objective is met through a review and evaluation of the most recent data on zirconium alloys and to identify the most important new information and discuss its significance in relation to fuel performance now and in the future. Included in the review are topics on materials research and development, fabrication, component design, and in-reactor performance presented in conferences, journals and reports.

The primary issues addressed in the review and this report is zirconium alloy research and development, fabrication, component design, ex- and in-reactor performance including:

- Regulatory bodies and utility perspectives related to fuel performance issues, fuel vendor developments of new fuel design to meet the fuel performance issues.
- Fabrication and Quality Control (QC) of zirconium manufacturing, zirconium alloy systems.
- Mechanical properties and their test methods (that are not covered in any other section in the report).
- Dimensional stability (growth and creep).
- Primary coolant chemistry and its effect on zirconium alloy component performance.
- Corrosion and hydriding mechanisms and performance of commercial alloys.
- Cladding primary failures.
- Post-failure degradation of failed fuel.
- Cladding performance in postulated accidents (Loss of Coolant Accident (LOCA), Reactivity Initiated Accident (RIA)).
- Performance of accident tolerant fuel (ATF)
- Dry storage.
- Potential Burn-up (BU) limitations.
- Current uncertainties and issues needing solution are identified throughout the report.

Background data from prior periods have been included wherever needed. The data published in this Report is only from non-proprietary sources; however, their compilation, evaluations, and conclusions in the report are proprietary to ANT International and ZIRAT/IZNA members as noted on the title page.

The authors of the report are Dr. Charles Patterson, Dr. Ronald Adamson, Dr. Kit Coleman, Dr. Tahir Mahmood and Dr. Albert Machiels-

The work reported herein will be presented in four Seminars:

- February 19-21, 2018, Clearwater Beach, Fl., USA
- March 12-14, 2018, Palma de Mallorca, Spain
- November, 2018 in China
- November, 2018 in Japan

The Term of ZIRAT22/IZNA17 started on February 1, 2017 and ends on March 31, 2018.

All literature that we refer to in this Report is available in the ANT International Literature Database (LDB). Please contact Mr. Peter Rudling at Peter Rudling peter.rudling@antinternational.com for more information.

2 Burnup and fuel technology achievements (Charles Patterson)

2.1 Introduction

The objective of this Section is to summarize the key performance issues that could affect fuel design, fabrication or operation of nuclear fuel in the near or longer terms. Topics covered relate primarily to the fuel itself but also include a brief review of small modular reactors. The information sources reviewed, screened and evaluated include nearly all the related publications and technical meeting presentations of the past, approximately 18 months. This Section is intended to be a guide to current issues related to these topics and to provide an alert to items that could affect fuel related operations. The extensive volume of information involved limits the presentations to the most significant features and conclusions, and the reader is urged to refer to the referenced publications for more detail.

2.2 Trends in fuel and reactor operating conditions

2.2.1 General trends

The driving forces in the evolution of fuel technology and operating conditions are improved fuel reliability and economics while maintaining acceptable margins to operating and regulatory safety limits. Driving forces also include improvements in margins to fuel damage thresholds and mitigation of the consequences of severe accidents. These forces provide incentives for significant advances in materials technology, software for designing and predicting fuel performance, sophisticated instrumentation, modifications in water chemistry and methods for post-irradiation examinations. These forces are also causing shifts in the utilization of nuclear power in established and developing nuclear countries. Activities related to accident tolerant fuel are reviewed in a separate section of the Annual Report.

Advances in technology have increased the demands on fuel performance levels and put pressure on regulatory agencies to license operations to increased burnup levels. The types of changes in LWR design and operating methods intended to achieve improved safety and economics have not changed in the past years and still include:

- Plant power uprates that range from 2 to ~20%,

- More aggressive fuel designs with a larger amount of fuel at or near the near-universal limit for civilian power reactors of 5% 235U,

- Increased concentrations and more widespread use of burnable neutron absorbers,

- More aggressive fuel management practices, with increased power peaking factors and increased amounts of fuel operating closer to design limits,

- Annual fuel cycles extended to 18 and 24 months,

- Increased discharge burnups as high as 64 GWd/MT batch average exposures by means of higher enrichments, increased amounts of burnable absorbers in the assemblies (absorber concentrations and number of rods with neutron absorbers) and, in PWRs, higher lithium and boron levels or enriched boron in the coolant,

- Development of cladding and fuel assembly materials with increased resistance to corrosion, hydrogen pickup and radiation growth,

- Reduced activity transport by Zn injection into the coolant,

- Improved water chemistry controls and increased monitoring,

- Component life extension with hydrogen water chemistry (HWC), noble metal chemistry (NMC) and more extensively with on-line noble metal chemistry (OLNC) in BWRs.

A combination of environmental, economic, social and political issues are contributing to changes in the worldwide application of nuclear power. At the beginning of 2017, the International Atomic Energy Agency reported 448 operating nuclear power reactors with a total installed electrical generating capability of 391.7 GWe[1], [IAEA, 2017]. The number of reactors with operational status and the associated generating capacities are shown by country in Figure 2-1. The number is changing due to the closure of plants in some countries and the startup of new plants in others. Ten reactors started operation and three were closed down, resulting in a net increase in nuclear capacity of just over 8 GWe. The amount of electricity supplied by nuclear globally increased 2476 TWeh in 2016 as shown in Figure 2-2. The installed capacity of the U.S., France, Japan, China, Russia and the Republic of Korea accounts for approximately 70% of the total nuclear generating capability.
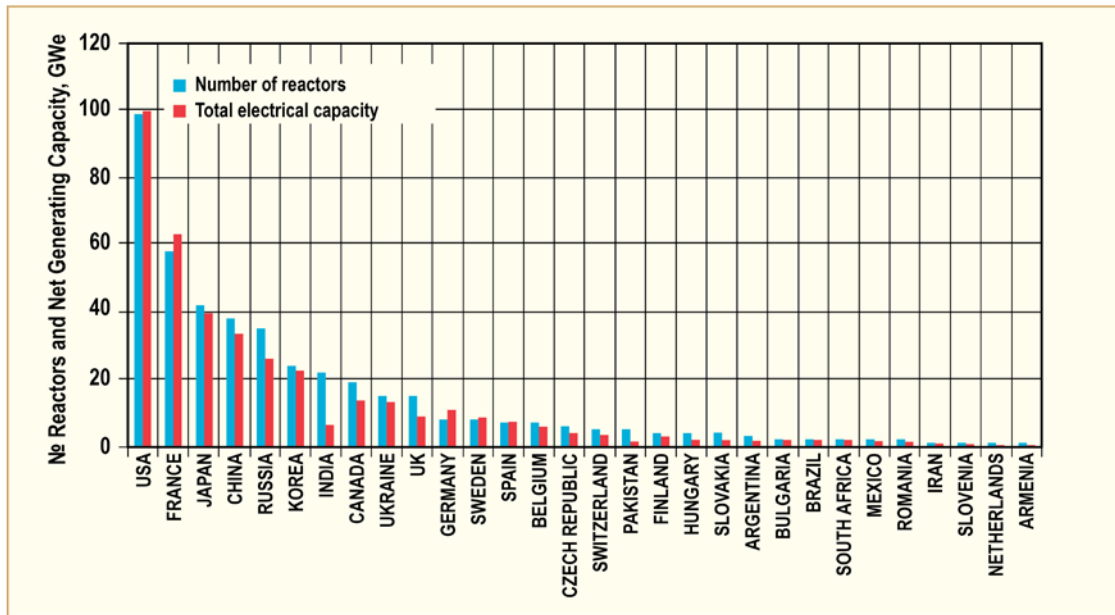
Figure 2-1:   Electrical generating capabilities of nuclear reactors by country, after [IAEA, 2017].

[1] The Power Reactor Information System (PRIS) database of the IAEA includes experience of all nuclear countries. Information compiled in PRIS through the end of 2016 is used as a primary source for information in this section. Although the database is updated at frequent intervals, information in PRIS can differ from regional databases and other periodic tabulations due to the timing of the updates.
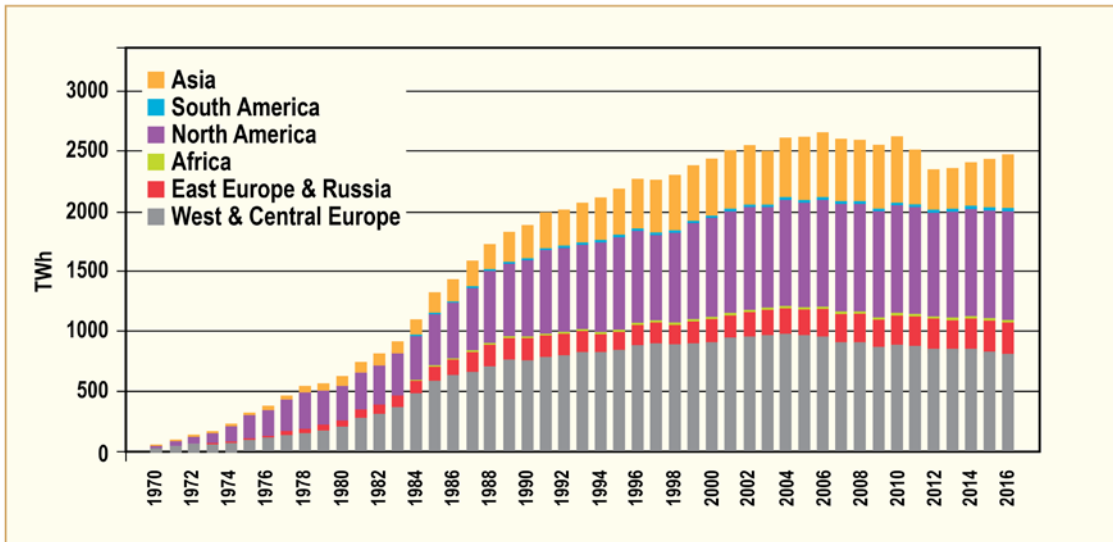
Figure 2-2:   Nuclear generating capacity by year and region, [WNA, 2017d].

The energy produced by the existing fleet of nuclear reactors constitutes about 10% of the worldwide energy production and about 23% in countries with nuclear power plants,[WNA, 2016] and [IAEA, 2016a]. However, as shown in Figure 2-3, the relative role of nuclear power varies markedly among countries; e.g., 72% of electrical power is produced by nuclear reactors in France and 2% in Japan. The large generating capacity (Figure 2-1) and large nuclear fraction in France (Figure 2-3) represents the historic policy of this country. The large capacity and the small production fraction in Japan represents the lingering effects of the 2011 Tohoku earthquake and tsunami; i.e., continued plant shutdowns with ongoing assessments of nuclear and plant safety by the utilities, regulators and politicians. The large generating capacity and small nuclear share in the U.S., China and Russia reflects the reliance of these countries on alternate sources of energy – primarily fossil fuels, but with increasing amounts of energy from solar and wind sources.
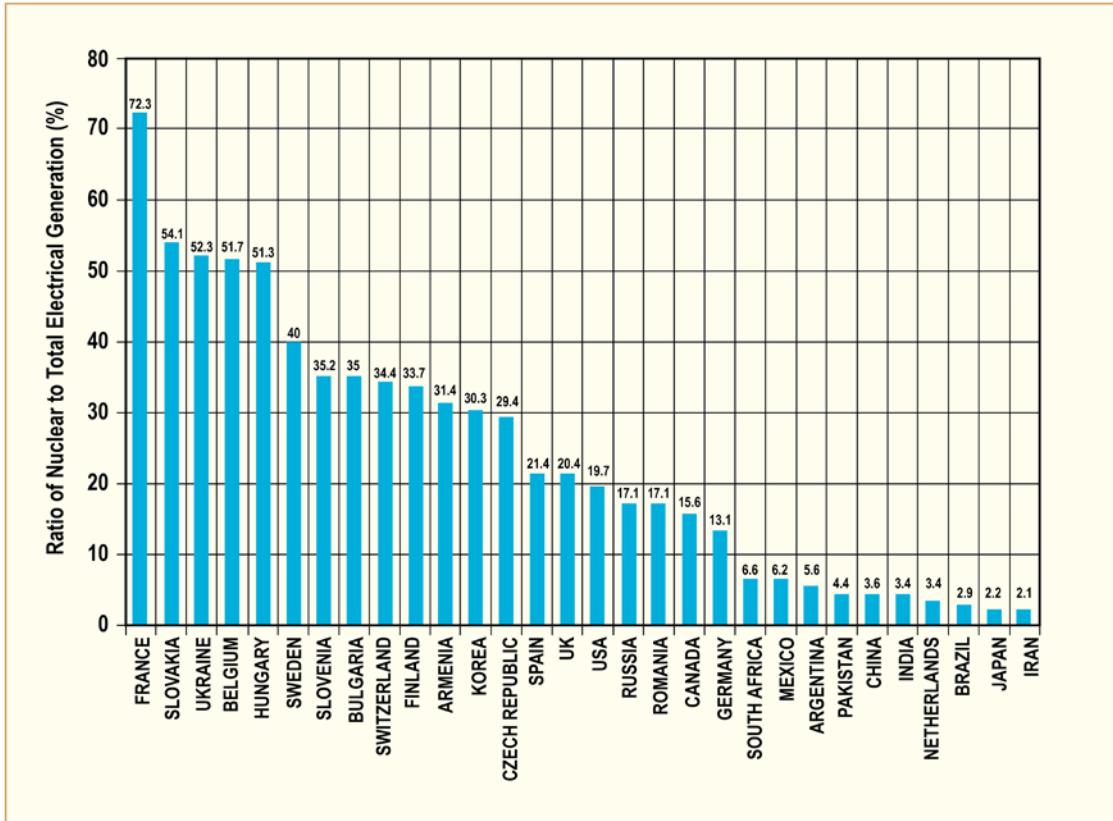
Figure 2-3:   Electrical production by nuclear power plants relative to the total electrical production by country in 2017, [IAEA, 2017].

Light water reactors continue to be the most commonly used source of nuclear energy. As shown in Figure 2-4, PWRs and VVERs constitute the greatest number of reactors and the largest generating capacity; viz., 289 out of 448 reactors and ~70% of the operable nuclear generating capacity. This condition is expected to continue since 50 of the 60 reactors currently under construction are PWRs or VVERs, [IAEA, 2016b].
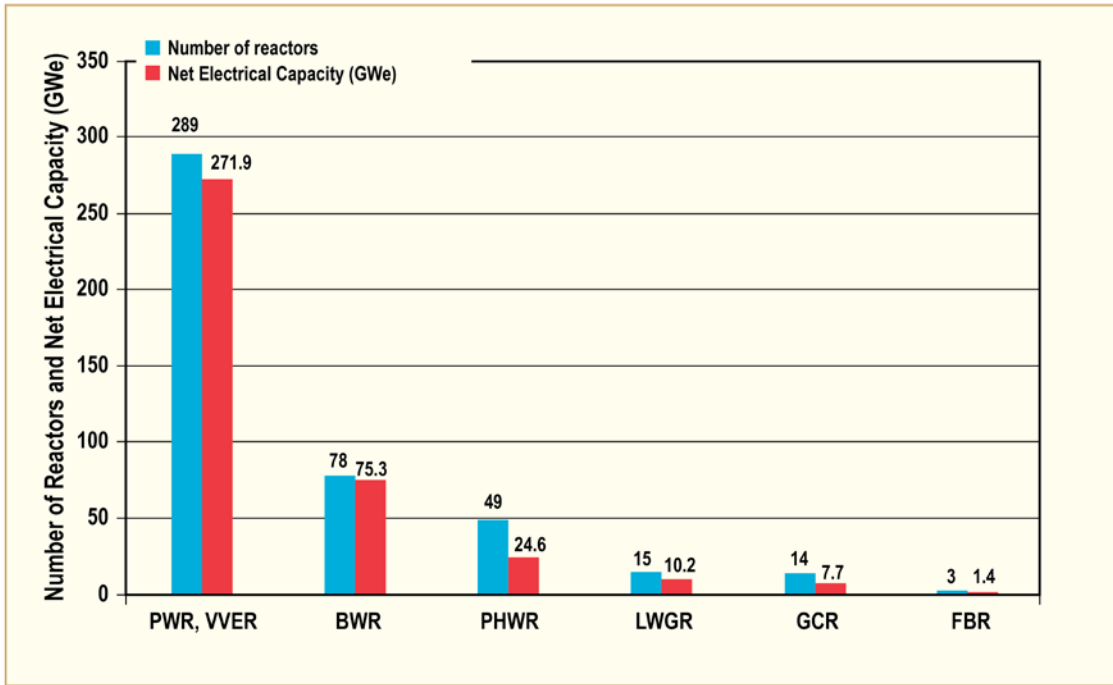
Figure 2-4:   Number of operating nuclear reactors and the net electrical generating capacity by reactor type, after [IAEA, 2017].

As shown in Figure 2-5 and Figure 2-6, a large number of new reactors are being constructed. The majority (84%) of the reactors currently under construction are PWRs or VVERs. Thirty three reactors (54% of the total number) are being built in China, Russia and India. The remainder are being built in the rest of Asia, Europe and North and South America.
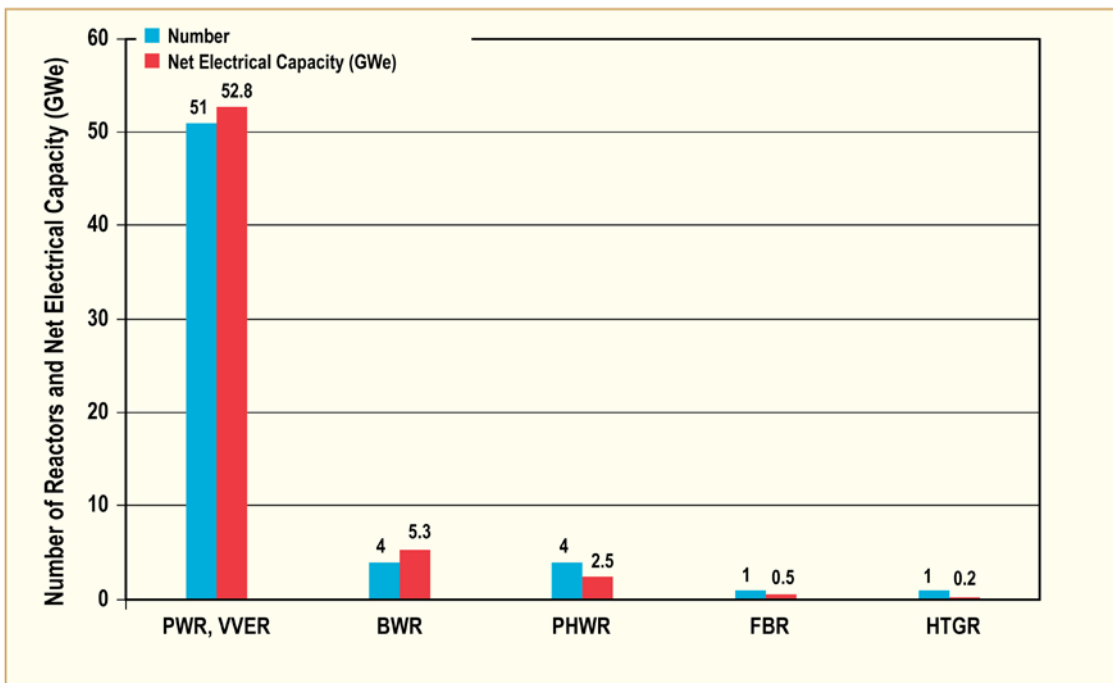
Figure 2-5:   Nuclear power plants under construction in 2016 by reactor type, after [IAEA, 2017].
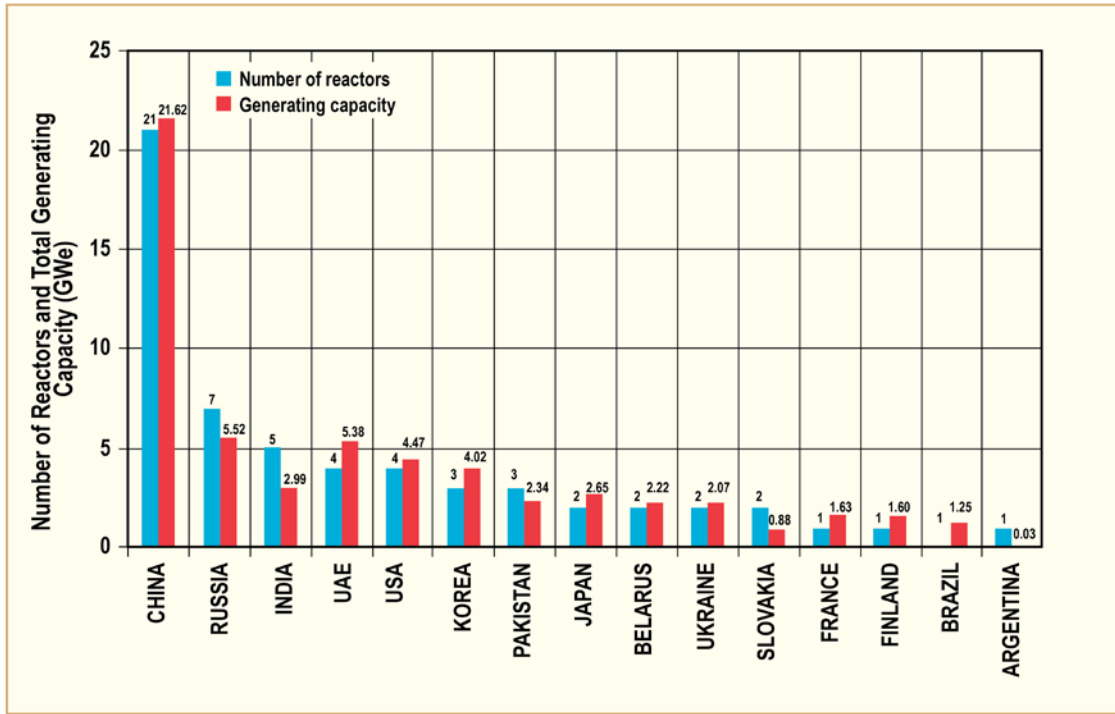
Figure 2-6:   Nuclear power plants under construction in 2016 by country, after [IAEA, 2017].

The age of the existing fleet of reactors is approaching the point at which life extension or plant shutdown will be needed (e.g., 40 years in the U.S.), Figure 2-7. The generating capacity corresponds closely to the number of plants as indicated in Figure 2-1. So, decisions regarding life extension or shutdown will affect both the number of plants and the contribution of nuclear to the total energy production of the affected countries.

Based on the capacity factor of NPPs relative to age, shown Figure 2-8, there is no degradation in performance as plants reach the end of their initial license. The original 40-year license interval was based on the amortization of capital expenditures combined with design and operational conservatism rather than an intrinsic limitation on reactor lifespan; [WNA, 2017b]. Experience has identified life-limiting factors, which have been or are being addressed, generally in the 30-40 year range of NPP age. Extensions of 20 years are now common in countries where sociopolitical and economic climates are supportive or at least not hostile to nuclear power. Most NPPs in the U.S. (89 out of 99 plants) have already extended their licenses to 60 years, with five more license extensions being evaluated by the NRC in 2017; [WNA, 2017b]. In addition, the NRC is preparing to consider license extensions to 80 years. The license renewal process in the U.S. typically costs $16-25 million and requires 4-6 years for review by the NRC.

3 Microstructure and manufacturing

No new data presented this year.

4 Mechanical properties and fabrication (Kit Coleman)

4.1 Introduction

In this section we will discuss strength, deformation and ductility. Strength is expressed in terms of properties like yield strength. Deformation and ductility are expressed in terms such as elongation at fracture or strain-to-some limit for a particular loading condition. Fracture resistance is a combination of strength and ductility that describes the conditions to initiate and grow cracks and estimate the point of crack instability. Each of these properties is affected by their alloy composition and fabrication route, and by the consequences of their residence in a nuclear reactor in hot water. Neutron irradiation changes the microstructure thereby affecting the mechanical properties. For example, <a>-dislocation loops strengthen zirconium but when annihilated by strain, ductility and fracture toughness are reduced. Corrosion adds an oxide layer and produces hydrogen, some of which is picked-up by the components. Hydrogen is important because it forms hydrides that can lead to embrittlement. During fission, extra gasses are formed adding to the internal pressure inside a fuel rod that is important during LOCA and spent fuel storage. Vibrations between touching surfaces can produce wear and fretting that may be so severe that protective membranes are breached. All these changes have to be accommodated to assure that components function as designed. Often each of the properties is studied separately but provide input to computer codes to explain experiments and guide assessments for fuel performance. The fabrication of the components may be changed to meet special requirements. Large development programmes are considering accident tolerant fuel, including changes to current zirconium alloys. Contributions to some of these items were made during the year with a notable emphasis on hydrogen effects. Examples are summarised in the following sections.

4.2 Fabrication

4.2.1 Response of Zr-1Nb to simulated LOCA

The Zr-Nb alloys were originally developed in Russia based on Zr refined by an electrolytic process; for fuel cladding the alloy was Zr-1Nb and called E110. Subsequently the same alloy was made in France from Zr refined by the Kroll process and called M5. One difference between these versions of Zr-1Nb is in the trace concentration of halogens, F in E110 and Cl in M5. The fracture toughness of the sister alloy Zr-2.5Nb made from Kroll metal is very sensitive to traces of Cl [Aitchison & Davies, 1993] and is vacuum melted up to four times to minimise Cl concentration and much improve toughness – the initial Cl concentration in the sponge Zr is reduced from 0.019 at.% to 0.00013 at% by melting four times with a subsequent increase in crack growth resistance, dJ/da, from 150 MPa to 400 MPa [Theaker, et al., 1994]. A similar exercise with Zr-2.5Nb made from electrolytic powder produced a reduction in F concentration but without a subsequent improvement in crack growth resistance, Figure 4-1 [Coleman et al., 2006; Douchant, 2017]. The difference in behaviour is caused by the different configuration of two halogens; the Cl traces tend to form as two-dimensional sheets within the microstructure that lead to easy crack propagation whereas the F traces form three-dimensional particles up to 1 μm in diameter that lead to ductile cavities. The concentration of F is important in E110 cladding when evaluated after exposure to LOCA conditions [Markelov, et al., 2017]. 30 mm long sections of cladding were held in steam between 1000 and 1200 °C for times up to 5000 s.
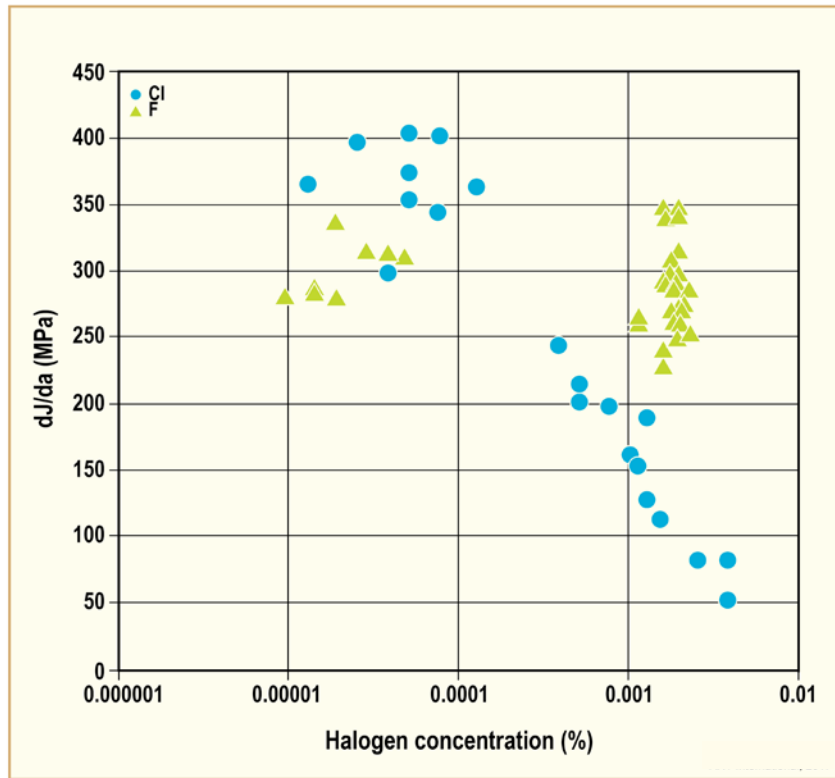
Figure 4-1:   Dependence of crack growth resistance on concentration of halogens in Zr-2.5Nb [Coleman et al., 2006; Douchant, 2017]

During fabrication, the Zr-1Nb source material was melted 2, 3 or 4 times resulting in a reduction in F concentration. As a consequence, at 1000 °C the time to breakaway oxidation increased and hydrogen pickup was reduced at the same oxide thickness, normalised to 17% equivalent cladding reacted (ECR). The residual ductility at 20 °C after quenching from high temperature was measured in ring compression tests. After time at 1000 °C, the residual ductility for quadruple melted material varied from 1.5 to 7% while that of the double melted material was very low, 0.1 to 0.2%. The benefits of multiple melting are apparent after exposure to 1000 °C steam, Table 4-1, but the benefits are lost after exposure at 1200 °C. Now the double melted material had the largest residual ductility, around 3%, although with still the highest hydrogen pickup, 27 to 35 ppm, whereas the quadruple melted material had the lowest residual ductility, 1 to 1.4%, and lowest hydrogen pickup, 5 to 6 ppm.

Table 4-1:   Reduction in fluorine concentration in E110 by multiple melting and the consequences for the response to exposure to steam at 1000 °C [Markelov et al., 2017].

Number of melts	Fluorine concentration (ppm)	Time to oxide breakaway (s)	Hydrogen pickup (ppm)	Residual ductility (%)
2	4 to 5	520	1780 to 1880	0.1 to 0.2
3	2 to 3	3930	27 to 96	0.4 to 1.0
4	<1	>5000	30 to 40	1.5 to 7.0
				© ANT International 2017

4.2.2 Development of Accident Tolerant Fuel – a response to Fukushima

In 2011 a major undersea earthquake off the eastern coast of Japan produced a large tsunami that inundated three operating reactors at Fukushima. The reactors shut-down as designed but the pumps and batteries used to supply emergency cooling water were destroyed causing a _s_tation _b_lack_o_ut (SBO). Rather than the _e_mergency _c_ore _c_ooling _s_ystem (ECCS) being in place within a few seconds, no cooling was available for many hours. In power reactors about 1% of full power is still available 4 h after reactor shut-down, and even after 10 d, 0.2% of full power has to be accommodated. As a consequence of this delay, the decay heat is not transported away, the fuel is no longer protected and melts releasing large quantities of highly radioactive material so large radiation fields develop in the reactor building. Section 4.5, [ZIRAT 19, 2014], provides a description of such problems at Fukushima. The responses of the nuclear industry included devising mobile cooling systems, improved reactor siting plans and defence systems, and development of _a_ccident _t_olerant _f_uel - ATF. For the latter, the uranium alloy may be changed from UO_2 to, for example, variations of U-Si. Changing the basic cladding material has been suggested, for example, SiC-composites or Fe-Cr-Al-(Si-N), but ATF using cladding based on zirconium alloys protected by a surface coating is also being explored. The key requirements are to minimise hydrogen generation and heating in the reactor core from oxidation during the coping time after the loss of cooling, while not sacrificing the current good performance properties during normal operation, gained over the past 60 years. Improved resistance to creep deformation and cracking at high temperatures would also be desirable to retard ballooning and minimise spalling of prospective coatings. Avoiding severely disrupting current fabrication practice is considered a great advantage if a simple modification to existing zirconium alloy cladding could be shown to be effective in extending coping time. Licensing such fuel should be straightforward. A summary of the development plans and requirements for ATF are listed in [Zinkle et al., 2014; Bragg-Sitton, 2014; Duan et al., 2017, and Karoutas et al., 2018]. Chapter 9 of this report provides a comprehensive description of the world-wide project to develop fuel that can withstand extensive SBO with the current (or better) reactor performance during normal operation and with little increase in cost and complexity in fabrication. As part of the review on fabrication processes, we briefly discuss some of the methods that retain the initial zirconium alloy cladding. Here the proposed methods involve coating the surfaces. The inside surface of the cladding also requires protection since any breach in the cladding during SBO would lead to a similar problem to the one being solved for the outer surface.

Several methods are proposed for coatings zirconium alloys but variations on Physical Vapour Deposition (PVD), Chemical Vapour Deposition (CVD) and Cold Spraying (CS) are probably the most amenable to application for fuel cladding since the temperatures of application are usually lower than those for stress relieving. Three examples follow.

4.2.2.1 Physical vapour deposition (PVD)

Physical vapour deposition describes a variety of vacuum deposition methods that can be used to produce coverings with a wide range of thicknesses. PVD is characterized by a process in which the material goes from a condensed phase to a vapour phase and then back to a condensed phase as a thin film. The most common PVD processes are sputtering and evaporation. Figure 4-2 is a schematic diagram of a typical process.

Plate specimens of Zircaloy-2 (30 mm x 10 mm x 1 mm) were coated with CrN using PVD to a layer thickness between 2 to 4 μm. Some of the specimens were deliberately scratched to simulate operational damage. They were corroded for up to 120 d at 300 °C in D_2O with pH of 10.4 controlled by LiOH and in steam at 500, 750 and 1000 °C for 1 h [Daub et al., 2017]. At low temperature the CrN layer reduced the deuterium pickup by a factor of three, except where the layer was damaged and protection was lost and extra deuterium was picked up. The layer was protective at high temperatures except when the layer was damaged or in positions where adhesion had been lost, Figure 4-3.
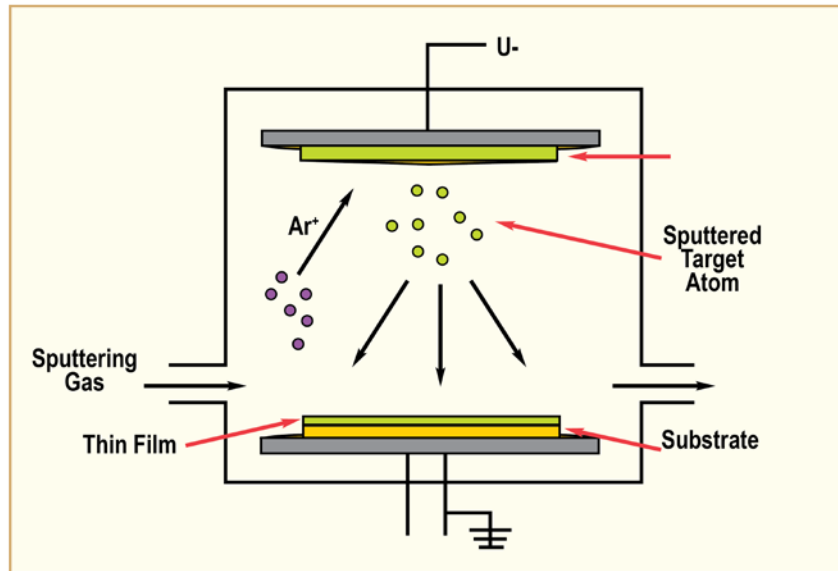
Figure 4-2:   Sputtering of target metal by Ar ions and deposition on a substrate.
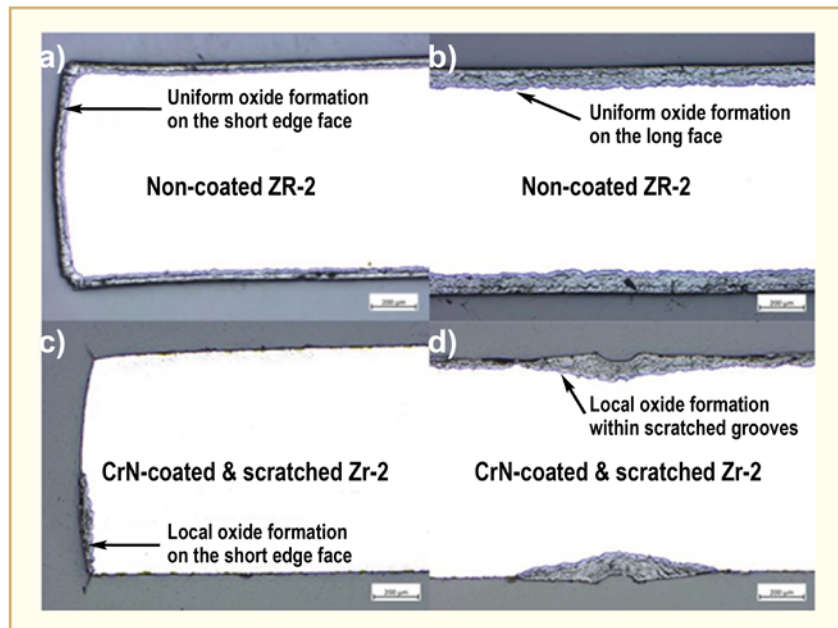
Figure 4-3:   Light microscopy of cross-section of plate specimens of Zircaloy-2 exposed to 1000 C steam for one hour: a,b) non-coated Zircaloy-2 and c, d) Zircaloy-2 coated with CrN and scratched [Daub et al., 2017].

4.2.2.2   Chemical Vapour Deposition (CVD)

CVD relies on chemical processes between one or more volatile precursors that react with the substrate to be protected, Figure 4-4. Subsequent volatile by-products have to be removed by gas flow through the reaction chamber.
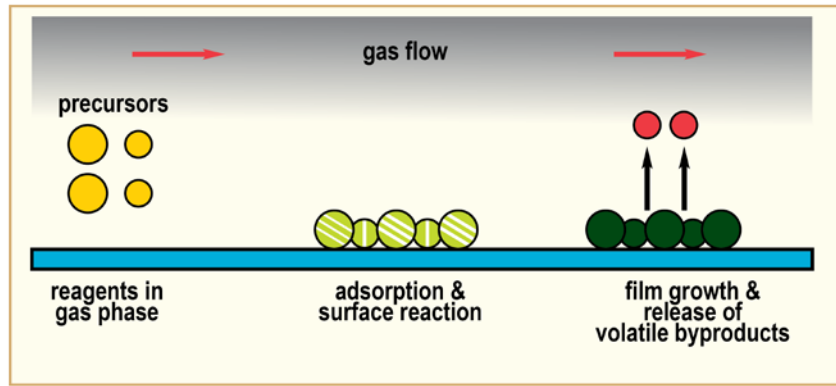
Figure 4-4:   Schematic diagram of chemical vapour deposition on a substrate – blue band.

Coating both surfaces of fuel cladding by CVD is being studied so the inside surface may also be protected against SBO [Michau et al., 2017]. The proposed coating is based on chromium carbide with a composition close to Cr_7C_3. The precursor is a metalorganic that decomposes around 400 °C. It is diluted in toluene. The solution is injected into a flash vaporization chamber to generate a reactive vapour and transported by a carrier gas to the CVD reactor. The pulsed injection system divides the liquid solution into a cloud of small droplets, the vaporisation step. The vapour is thermally decomposed inside the reactor using an oven. The product of decomposition is deposited as an amorphous layer on test specimens and inside a 1 m length of fuel cladding.

The growth of the film thickness was simulated through calculations of mass transport and rates of reaction of the decomposition processes. The model agreed well with observations of film thickness after injection of the precursor from one end at 400 °C and a pressure of 0.67 kPa, Figure 4-5(a). The calculations suggest that to achieve a uniform thickness along the full 1 m length of the model fuel cladding would require a successive injection from both ends and a reduction in reaction temperature and pressure, Figure 4-5(b).

In oxidation tests at 1200 °C in wet-air, catastrophic oxidation was postponed for 1.5 h with a coating thickness of 9 μm although a coating of only 2 μm was ineffective. In tests where coated specimens were heated to 1100 °C for several minutes followed by water quenching, all the coatings remained protective apart from a few small cracks. Figure 4-6 shows a depth profile analysis using Glow Discharge Optical Emission Spectroscopy (GDOES) and a SEM cross-section of the sample, after the oxidation and quenching. GDOES profiles exhibit a succession of layers from the surface to the substrate: surface chromium oxide, partially oxidized coating, non-oxidized coating, inter-diffusion between coating and Zr and finally the non-oxidized substrate. X-ray diffraction analyses confirmed the formation of Cr_2O_3 and the non-oxidized substrate. ZrC had formed because of inter-diffusion and the non-oxidized initially amorphous Cr_3C_2 coating had crystallized. The analysis confirmed that oxygen diffusion was also prevented.
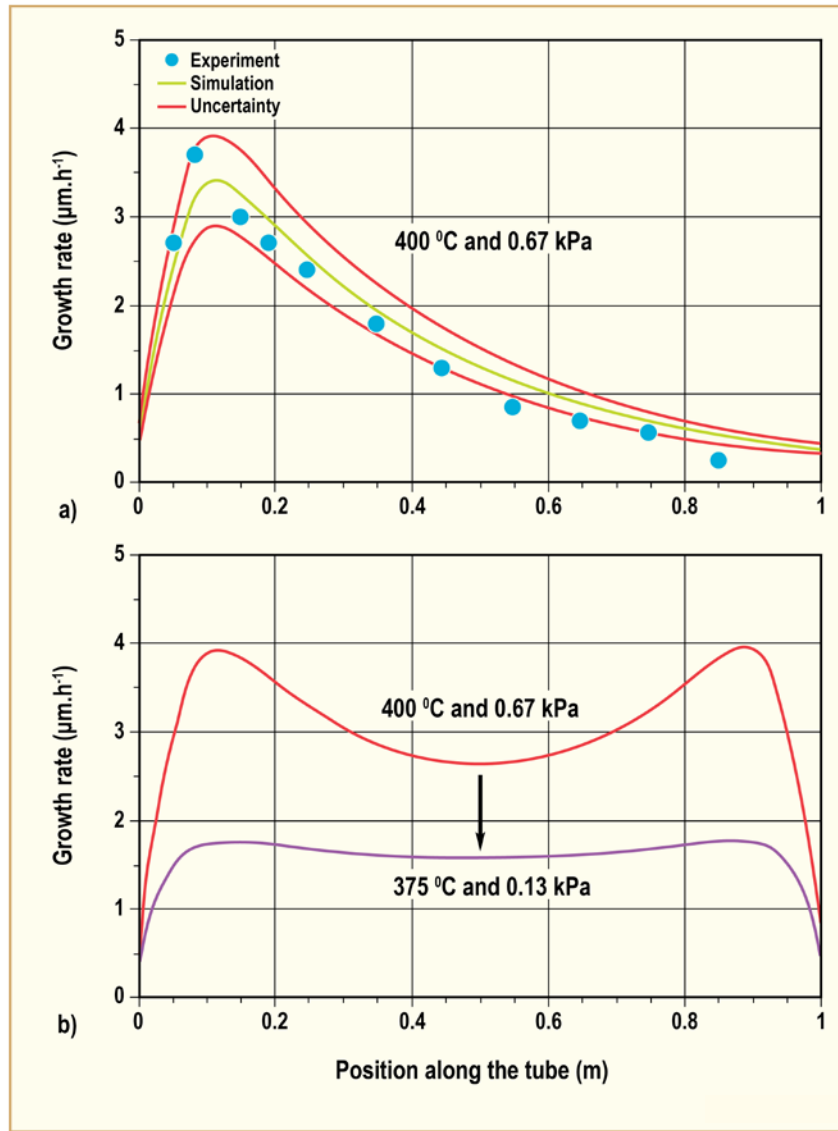
Figure 4-5:   Optimization of CrC film thickness uniformity along a 1 m fuel cladding tube section: (a) Comparison of simulated and measured profiles of growth rates with a single precursor injection only from the left end; (b) Calculated growth rates profiles with two successive precursor injections, one from each side, under two conditions for injection [Michau et al., 2017.]
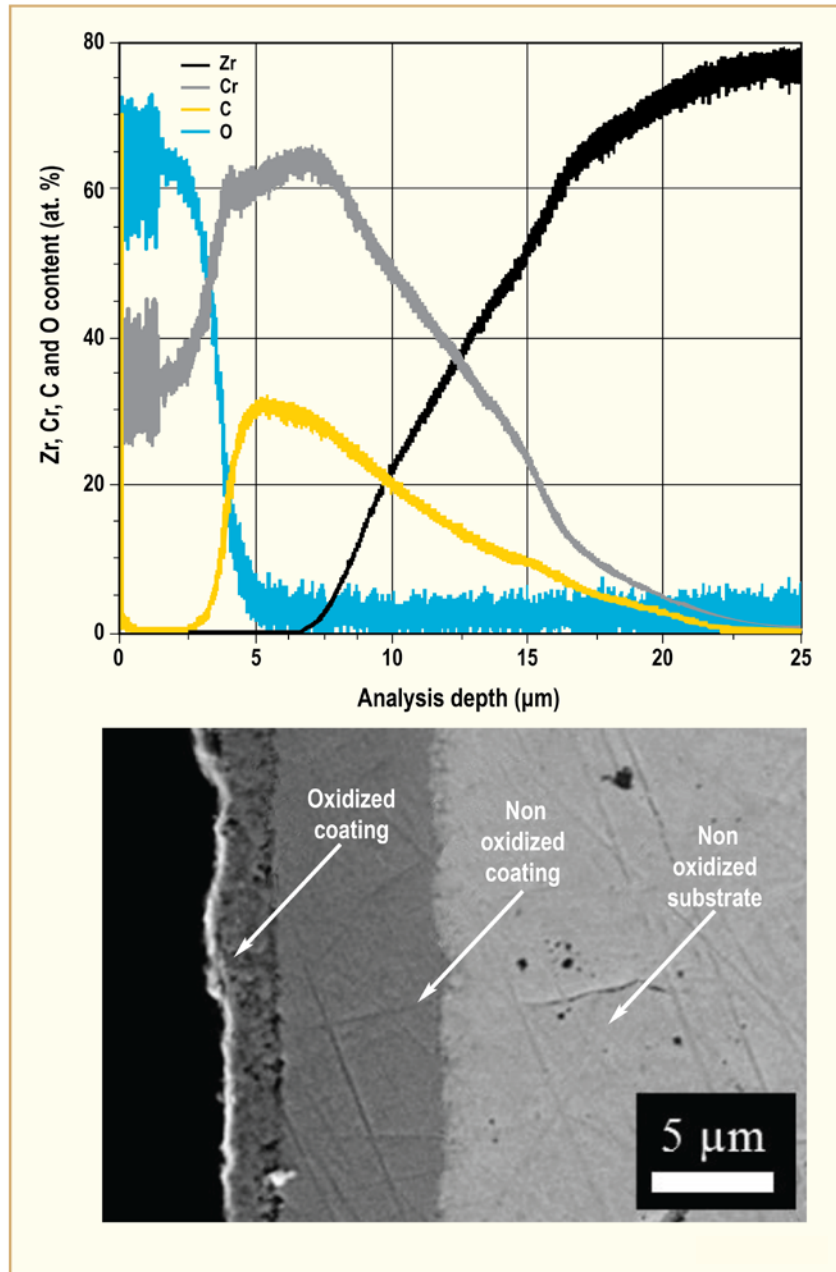
Figure 4-6:   GDOES and SEM analyses of the 9 μm Cr_xC_y coated Zircaloy-4 plate after 14 min at 1100 °C in dry air followed by water quenching [Michau et al., 2017.]

4.2.2.3   Cold spraying (CS)

The cold spray process, as shown schematically in Figure 4-7, imparts supersonic velocities to metal particles by placing them in a heated nitrogen or helium gas stream that is expanded through a converging–diverging nozzle. The powder feed is inserted at high pressure at the nozzle entrance. High pressures and temperatures yield supersonic gas velocities and high particle acceleration within the gas stream. The particles, entrained within the gas, are directed towards the surface, where they embed on impact, forming a strong bond with the surface. The term "cold spray" has been used to describe this process due to the moderate temperatures (100-500°C) of the expanded gas stream that exits the nozzle. Subsequent spray passes increase the structure thickness. The adhesion of the metal powder to the substrate, as well as the cohesion of the deposited material, is accomplished in the solid state.
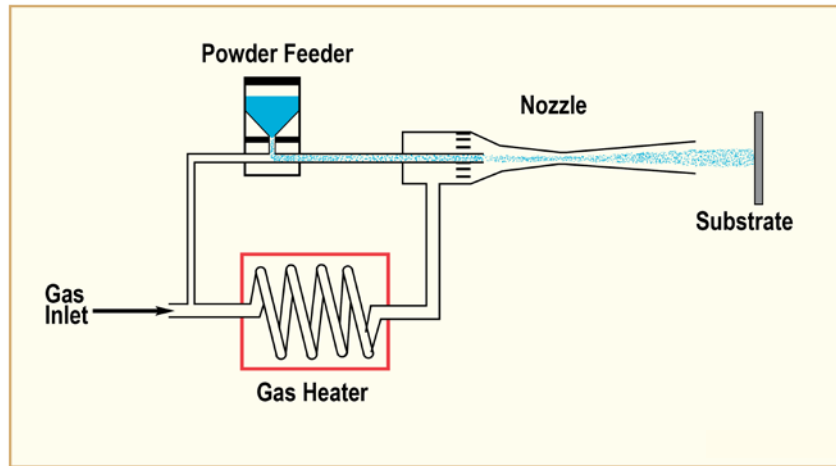
Figure 4-7:   Typical Cold Spray Assembly

Figure 4-8 depicts the sequence of a particle contacting the substrate. Upon impact with the substrate surface, the particle flattens while the substrate crater depth and width increase. At the same time, a jet composed of both the particle material and the substrate material is formed at the particle/substrate contact surface. Simultaneously, there is a temperature rise, confined to the particle/surface interface. This temperature rise is an indication of shear instability, which causes extensive flow of material at the corresponding surfaces. The attributes of the cold spray process are low temperature deposition, a dense structure, and minimal or compressive residual stress in the surface. Usually the deposited material contains a porosity of less than 1% and possesses strength close to or above that of wrought material.
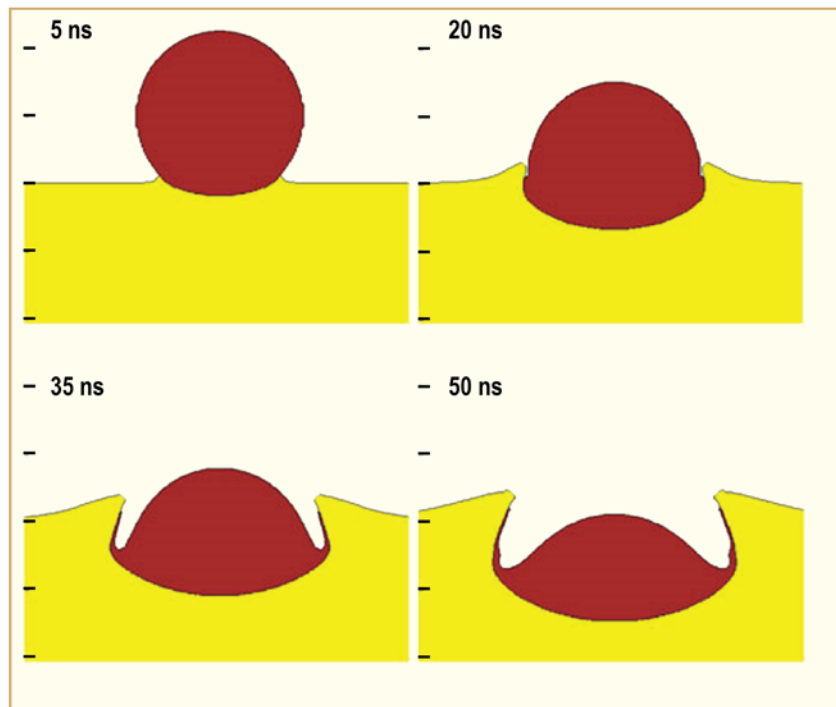
Figure 4-8:   Deformation of a spherical particle striking a substrate surface.

5 Dimensional Stability (Ron Adamson)

Unique aspects of material behavior in a nuclear power plant include the component's dimensional stability. In fast breeder reactors the Fe and Ni-based alloys creep and swell, that is, they change dimensions in response to a stress and change their volume in response to radiation damage. In water reactors, zirconium alloy structural components creep, do not swell, but do change their dimensions through the approximately constant volume process called irradiation growth. Radiation effects are not unexpected since during the lifetime of a typical fuel assembly component every atom is displaced from its normal lattice position at least 20 times. With very few exceptions, the mechanical and physical properties needed for reliable fuel assembly performance are affected by irradiation.

Practical effects of dimensional instabilities are well known and it is a rare technical conference in the reactor performance field that does not include discussions on the topic. In addition to lengthening due to irradiation growth, many components are subjected to creep stresses. Because of the difference in pressure inside and outside the fuel rod, cladding creeps down on the fuel early in life, and then creeps out again later in life as the fuel begins to swell. A major issue is to have creep strength sufficient to resist outward movement of the cladding if fission gas pressure becomes high at high burnups. PWR guide tubes can creep downward or laterally due to forces imposed by fuel assembly hold down forces or cross flow hydraulic forces – both leading to assembly bow which can interfere with smooth control rod motion. BWR channels can creep out or budge in response to differential water pressures across the channel wall, again leading toward control blade interference. Fuel rods, water rods or boxes, guide tubes, and tie rods all can lengthen due to irradiation growth, possibly leading to bowing problems. (For calibration, a recrystallised (RX or RXA) Zircaloy water rod or guide tube could lengthen due to irradiation growth more than 2 cm. during service; a cold worked/stress relieved (SRA) component could lengthen more than 6 cm.) Even RX spacer/grids could widen enough due to irradiation growth (if texture or heat treatment was not optimized) to cause interference with the channel.

In addition, corrosion leading to hydrogen absorption in Zircaloy can contribute to component dimensional instability due, at least in part, to the fact that the volume of zirconium hydride is about 16% larger than zirconium.

The above discussion leads to the concept that understanding the empirical details and mechanisms of dimensional instability in the aggressive environment of the nuclear core is important for very practical reasons. Reliability of materials and structure performance can depend on such understanding.

The sources of dimensional changes of reactor components (in addition to changes caused by mechanical loading, which is almost always in the elastic range, and conventional thermal expansion and contraction) are: irradiation growth, irradiation creep, thermal creep, stress relaxation (which is a combination of thermal and irradiation creep), and hydrogen and hydride formation.

Irradiation effects are primarily related to the flow of irradiation-produced point defects to sinks such as grain boundaries, deformation-produced dislocations, irradiation-produced dislocation loops, and alloying and impurity element complexes. In zirconium alloys, crystallographic and diffusional anisotropy are key elements in producing dimensional changes.

In the past, hydrogen effects have been considered to be additive to and independent of irradiation; however, recent data have brought this assumption into question. It is certain that corrosion-produced hydrogen does cause significant dimensional changes simply due to the 16-17% difference in density between zirconium hydride and zirconium. A length change of on the order of 0.25% can be induced by 1000 ppm hydrogen in an unirradiated material. Recent experiments indicate that the presence of hydrogen and/or hydrides does contribute to the mechanisms of irradiation growth but probably not creep.

Fuel rod diametral changes are dominated by stress dependent creep processes, as irradiation growth in the hoop direction is very small.

Fuel rod length changes are caused by several phenomena:

- Stress free axial elongation due to irradiation growth.

- Anisotropic creep (before pellet/cladding contact) due to external reactor system pressure. Because of the tubing texture, axial elongation results from creep down of the cladding diameter; however for heavily cold worked material, it has been reported that some shrinkage may occur. In a non-textured material such as stainless steel, creep down of the cladding would only result in an increase in cladding thickness, with no change in length.

- Creep due to pellet-cladding mechanical interaction (PCMI) that results from differences in the thermal strains between fuel pellets and cladding, pellet swelling and cladding creep (closure of the pellet-cladding gap) and that increases with the intensity of contact. PCMI begins early in life due to pellet cracking and relocation in the radial direction, is moderated by the effects of pellet densification and then increases after hard contact between the cladding and fuel. This occurs in mid-life of typical LWR fuel, depending on the cladding creep properties and the dimensional stability of the fuel, and early in life for PHWR (CANDU) fuel.

- Hydriding of the cladding due to corrosion.

Bow of a component such as a BWR channel or PWR control rod assembly can occur if one side of the component changes length more than the other side. Such differential length changes occur due to differential stress and creep, to relaxation of differential residual stresses, or to differential irradiation growth due to differences in flux-induced fluence, texture, material cold work, and hydrogen content.

Irradiation growth occurs simultaneously with irradiation creep if there is an applied stress. The two processes are generally assumed to be independent and additive, even though they compete for the same irradiation-produced defects mechanistically. When assessing dimensional changes of any component all sources of change must be taken into account. This is especially true for fuel rods, which will invariably have length-change components due to irradiation growth and anisotropic creep in addition to pellet-imposed stresses at higher burnups.

Irradiation creep was covered earlier by ZIRAT 14 Special Topic Report [Adamson et al., 2009], "Irradiation Creep of Zirconium Alloys" and Irradiation Growth is covered in the current ZIRAT 22 STR, "Irradiation Growth of Zirconium Alloys – A Review".

Since the ZIRAT 21 Annual Report [Adamson R. et al. 2016], there have been few papers on creep, and irradiation growth is covered thoroughly in the ZIRAT 22 STR [Adamson et al., 2017]. Therefore for the current ZIRAT 22 AR, just one paper will be reviewed as an example of how creep and growth data are used.

The paper is "The Performance of NSF in BWR Operating Conditions" [Cantonwine et al., 2017].

5.1 Boiling water reactor (BWR) channels

A square BWR channel surrounds (encases) the fuel bundle such that boiling is confined within the channel, with no (or little) boiling outside the channel. The cruciform-shaped control blade (CB) resides between four bundles, as shown in Figure 5-1. The channel defines the gap between the bundles where the CB inserts and withdraws to control the core criticality.
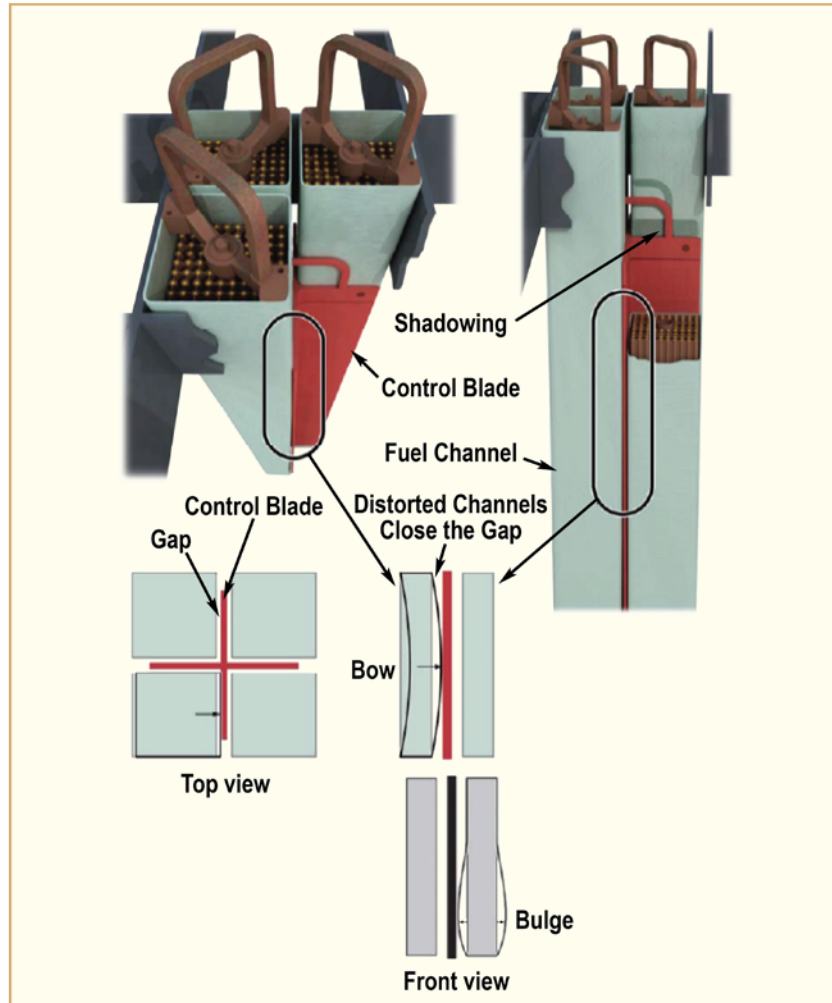
Figure 5-1:   Configuration of fuel bundles, channels and control blade in a typical BWR [Mahmood et al., 2010].

The key performance requirements of the channel are

1) dimensional stability, including both shape and thickness, and

2) adequate mechanical properties to withstand the applied stress created by pressure difference inside and outside the channel.

The distortion mechanisms identified by [Cantonwine et al., 2017] that affect dimensional stability are: fluence gradient bow (that is, gradient in irradiation growth on opposite channel sides); "shadow corrosion"-induced bow (that is, gradient of hydrogen on opposite channel sides); and bulge due to creep and elastic strain resulting from pressure differences inside and outside the channel.

Channel bow and bulge are illustrated in Figure 5-2 [Gorman & Lipsey, 1982], and in the lower right of Figure 5-1. It is seen that excessive bow or bulge can interfere with CB motion, thereby creating a potential safety issue.
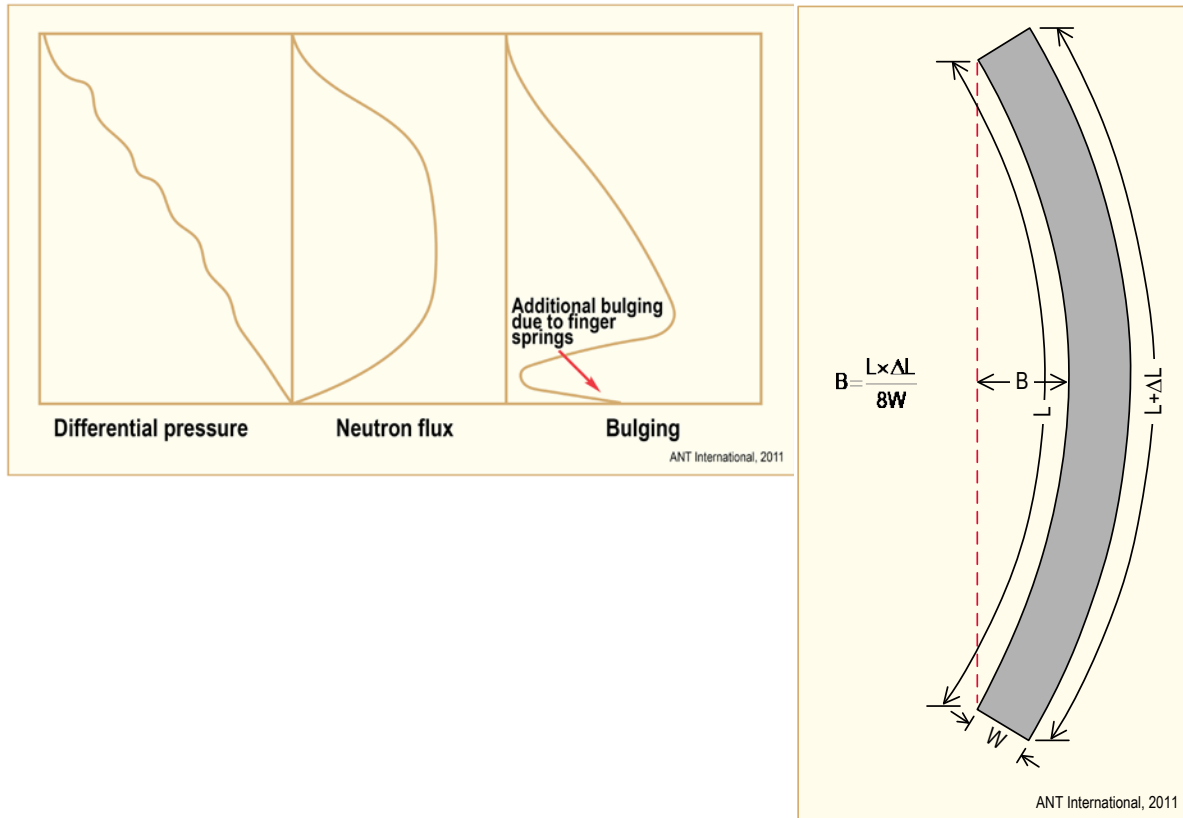
Figure 5-2:   Schematic diagrams of factors causing Bulge (left) and Bow (right) in typical square BWR channels. [Gorman & Lipsey, 1982]

Since Zircaloy-2 and, to a lesser extent, Zircaloy-4 channels have experienced bowing problems [Mahmood et al., 2010; Garzarolli et al., 2011], Global Nuclear Fuel-Americas (GNFA) has introduced a different material for channels, NSF. [Cantonwine et al., 2017] describe a qualification program that has resulted in USNRC approval of NSF channels for full reloads. That program is described in part here.

The composition of NSF (niobium-tin-iron) is given in Table 5-1, and is compared to similar alloys E635 and ZIRLO™. Heat treatment details are given in [Cantonwine et al., 2017; Garzarolli & Rudling, 2011].

Table 5-1:   Composition of Similar Alloys

Alloy	Composition, w/o Heat Treatment	
NSF	Zr1.0Sn1Nb0.40Fe	RXA
ZIRLO™	Zr1.0Sn1Nb0.10Fe	RXA/SRA
E635	Zr1.2Sn1Nb0.35Fe	RXA
		© ANT International 2017

5.2   Corrosion and hydriding

Corrosion of the Zr-Nb-type alloys depends on alloy heat treatment, as described for NSF by [Cantonwine et al., 2017]. In general, NSF has a higher corrosion rate than Zircaloy-2, Figure 5-3, and, as is the case for most Zr-Nb-type alloys, has a lower hydrogen pickup (HPU) and pickup

fraction (HPUF), Figure 5-4. For channels operated in symmetrical core locations, NSF had a HPU of 130 ppm with HPUF of 14% as compared to 200 ppm and 55% for Zircaloy-2.
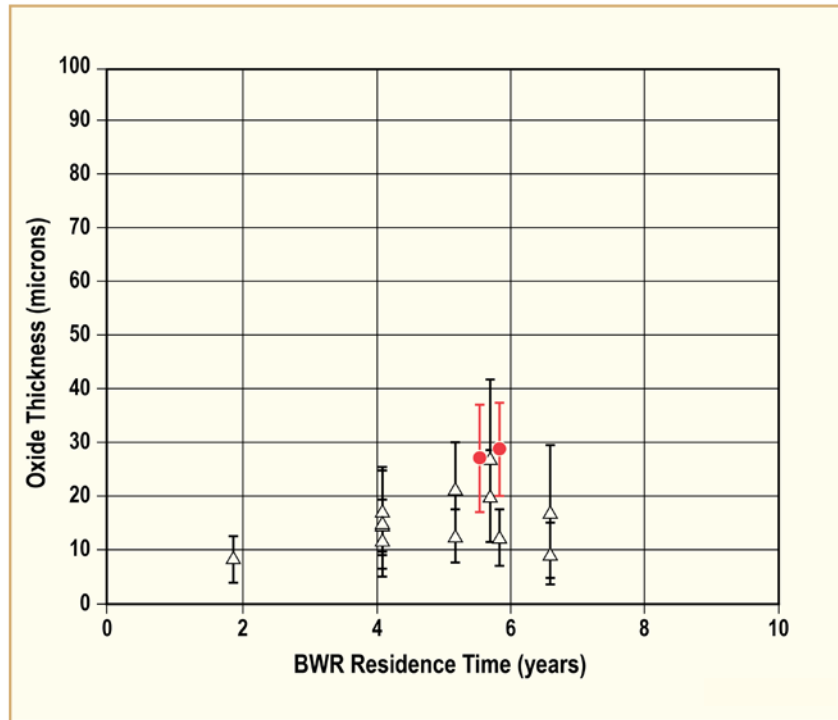
Figure 5-3:   Corrosion trend of BWR-irradiated NSF (red) and Zircaloy-2 (black) channel materials [Cantonwine et al., 2017].
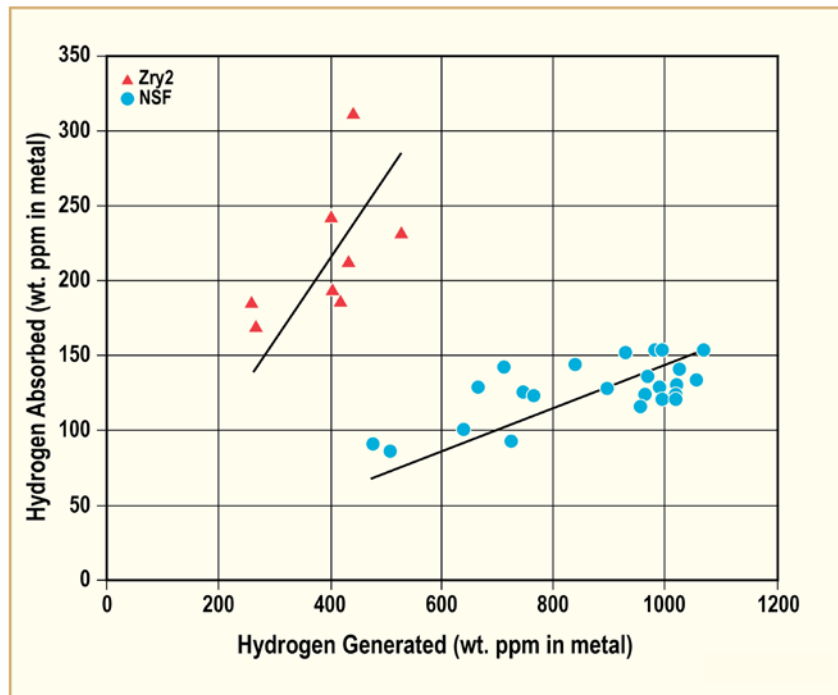
Figure 5-4:   Measured versus generated hydrogen for NSF and Zircaloy-2 channels with similar operations history [Cantonwine et al., 2017].

When control blades are inserted early in life ("controlled early in life"), shadow corrosion can develop on the outside surface of the channel next to the CB. Such increased corrosion has been linked

6 Corrosion and Hydriding

No new data presented this year. More data will be published in Zirat 23 Annual Report (2019)

7 Primary failure and secondary degradation

No new data presented this year. More data will be published in Zirat 23 Annual Report (2019)

8 LOCA, RIA

No new data presented this year. More data will be published in Zirat 23 Annual Report (2019)

9 Enhanced Accident Tolerant Fuels (Tahir Mahmood)

9.1 Introduction

Prior to the accident at Fukushima, the emphasis of advanced LWR fuel development was on improving nuclear fuel performance in terms of increased burnup for waste minimization, increased power density for power upgrades, and increased fuel reliability. In the aftermath of the 2011 East Japan earthquake, resulting tsunami, and subsequent damage to the Fukushima Daiichi nuclear power plants (Figure 9-1), nuclear power industry is at crossroads for both economic and political reasons. To keep nuclear energy a safe and competitive clean energy option, the industry has to innovate and find solutions to make it

- more resilient to unexpected events,

- economically viable (with respect to various alternate sources of energy, including renewable), and

- acceptable to the public (no adverse consequence for the environment, no matter what happens in or around a nuclear power plant).
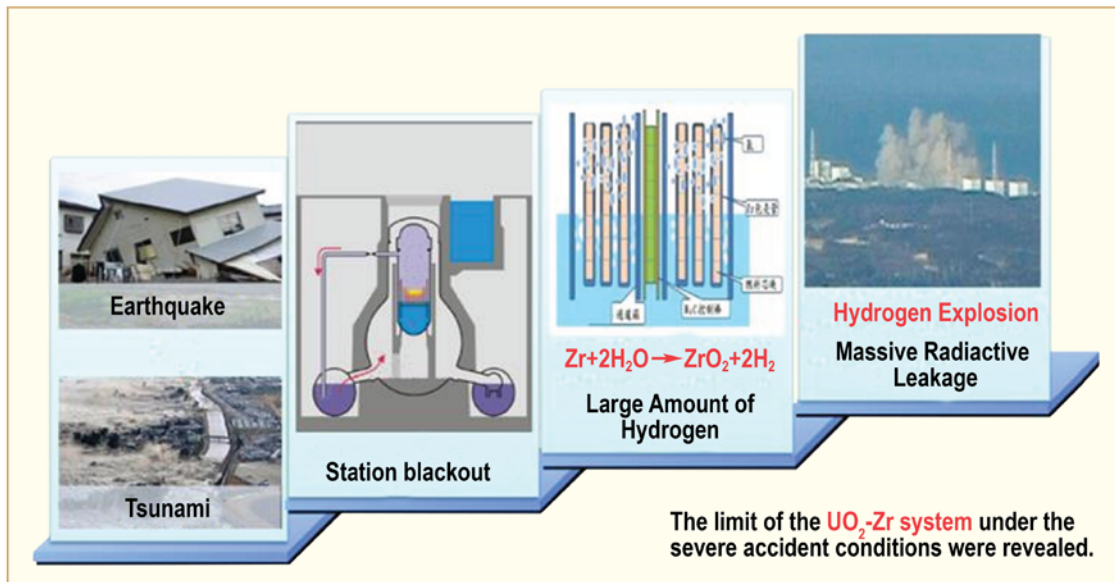
Figure 9-1:   Sequence of events at Fukushima Daiichi resulting in hydrogen explosion [Qiu, 2016].

Fukushima highlighted some undesirable performance characteristics of the standard fuel system during severe accidents, including accelerated hydrogen production under certain circumstances. Thus, fuel system behavior under design-basis accident and severe-accident conditions became the primary focus for advanced fuels, along with striving for improved performance under normal operating conditions to ensure that proposed new fuels will be economically viable.

Developing Enhanced Accident Tolerant Fuels (eATF) could be considered as one of the options to address the challenges. An eATF cladding that will survive in 1200-1500°C steam

- can extend the time without meltdown of the fuel,

- may significantly reduce the generation of hydrogen, and hence

- will provide additional coping time for operators to recover from the accident.

Any new fuel concept must be compliant with and evaluated against current design, operational, economic, and safety requirements. It is recognized that it will take a long time to develop and fully qualify an innovative fuel system. It is also noted that the potential benefits provided by these

advanced fuel systems are uncertain or difficult to evaluate, both in terms of safety margins restoration, and cost savings.

Among the multiple variants of eATF concepts under development all around the world (Figure 9-2) [Waeckel, 2017-1], the short term concepts have better chance to be used in the current nuclear power plants. The longer term fuel systems concepts (e.g. SiC/SiC cladding, refractory Molybdenum cladding, metallic fuels, micro-cells fuel, or uranium nitride fuel), despite their potential high level of performance in accident conditions, will need decades before they could be implemented on an industrial scale (i.e. beyond the expectation life of the current fleet).
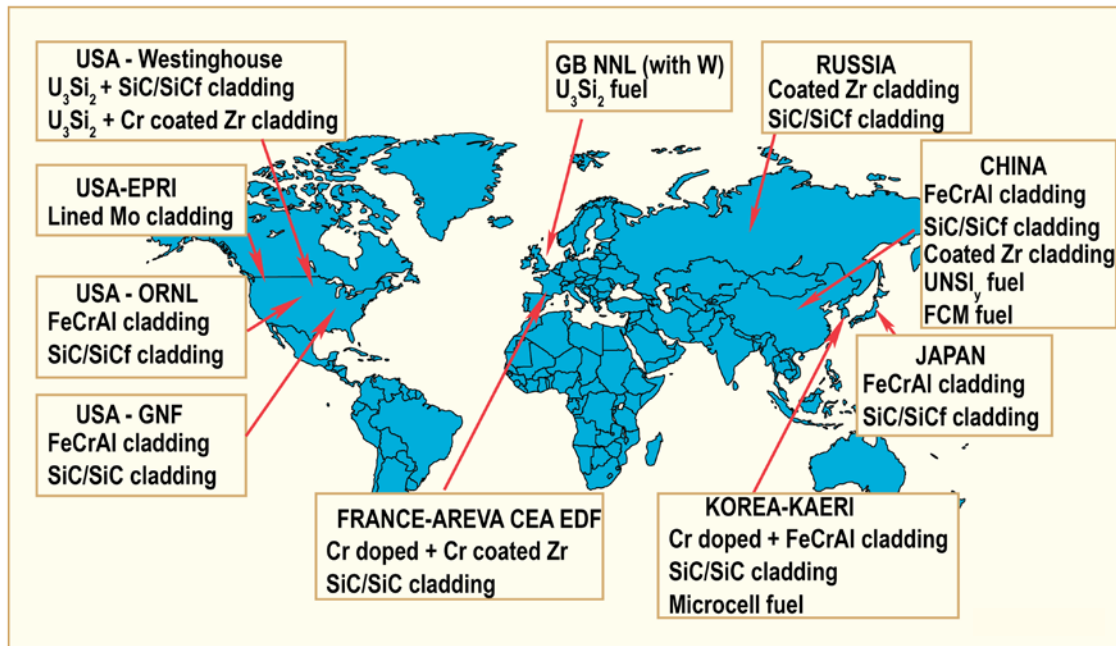
Figure 9-2:   Similar eATF concepts are under development all around the world [Waeckel, 2017-1].

The leading candidate technologies identified in Trade-off Study reported in [Barrett et al., 2012; Bragg-Sitton, 2014; Bragg-Sitton, 2015; Bragg-Sitton, 2016] include

- **eATF Cladding Designs**
  - Zircaloy-based
    - *Surface modified cladding*
    - *Coated cladding*
  - Advanced Metallic
    - *FeCrAl cladding*
    - *Mo-core composite cladding*
  - Ceramic
    - *SiC/SiC composite cladding*
  - *Co-extruded fuel*
- **eATF Fuel Designs**
  - Advanced/Enhanced UO2
    - *Improved μ-structure*
    - *UO2-based composites*
  - High fissile density

- U_3Si_2
- $UN-U_3S_{i2}$
- $UN-U_3Si_5$
    o Coated Particle-based
        - *Fully Ceramic Matrix (FCM)*

Each concept has some pros and cons across the spectrum of operating and transient conditions of interest. A systematic analytical and experimental evaluation is being performed during the feasibility studies.

To benefit the industry, it is judged that the normal time frame for material development and deployment must be reduced from decades to years. Development efforts have focused on the screening and characterization of material candidates with the highest degree of promise to produce a technically viable cladding in the shortest amount of time. The performance of these materials under accident conditions is such that potential exists for relaxation of safety system performance requirements, which in turn can result in substantial economic incentive for adoption of eATF. Therefore, several large eATF development programs are being pursued around the world.

The material test reactors that are being/will be used for irradiation testing of proposed ATF systems include ATR and TREAT at Idaho National Laboratory, HFIR at Oak Ridge National Laboratory, Halden reactor in Norway, OSIRIS at CEA, Saclay and material test reactors in many other countries like Korea, China, Japan, and Russia.

Independent of the outcomes of the current investigations, it is important to mention that developing eATF is a motivating driver for the entire nuclear fuel community, including young engineers and researchers. Thanks to the countless eATF related research projects, significant progress is being made towards

- Physical understanding of the fuel behavior under irradiation
- Advanced techniques to better analyze data and
- Developement of advanced calculations tools and methods.

The eATF development is still at the lab scale level. Before implementing a new type of fuel on an industrial scale, utilities and regulators will require to collect trouble free in-reactor data over a long period of time (i.e. from 6 to 10 years to cover the entire burnup range) and a successful qualification PIE program on irradiated specimens.

New Results - 2017

9.2   ATF development programs in USA

After Fukushima, enhanced accident tolerance became a priority topic. The US congress approved funding to DOE to start developing nuclear fuel with enhanced accident tolerance. Aggressive ten year schedule started in 2012 that has three phases [McCaughey, 2017].

- Phase 1: Feasibility is complete
- Phase 2: eATF development and qualification started in October 2016
- Phase 3: DOE insertion of LTR/LTA in commercial reactor by 2022 (industry is working to further accelerate this schedule)

The ten year schedule is shown in Figure 9-3 [McCaughey, 2017].
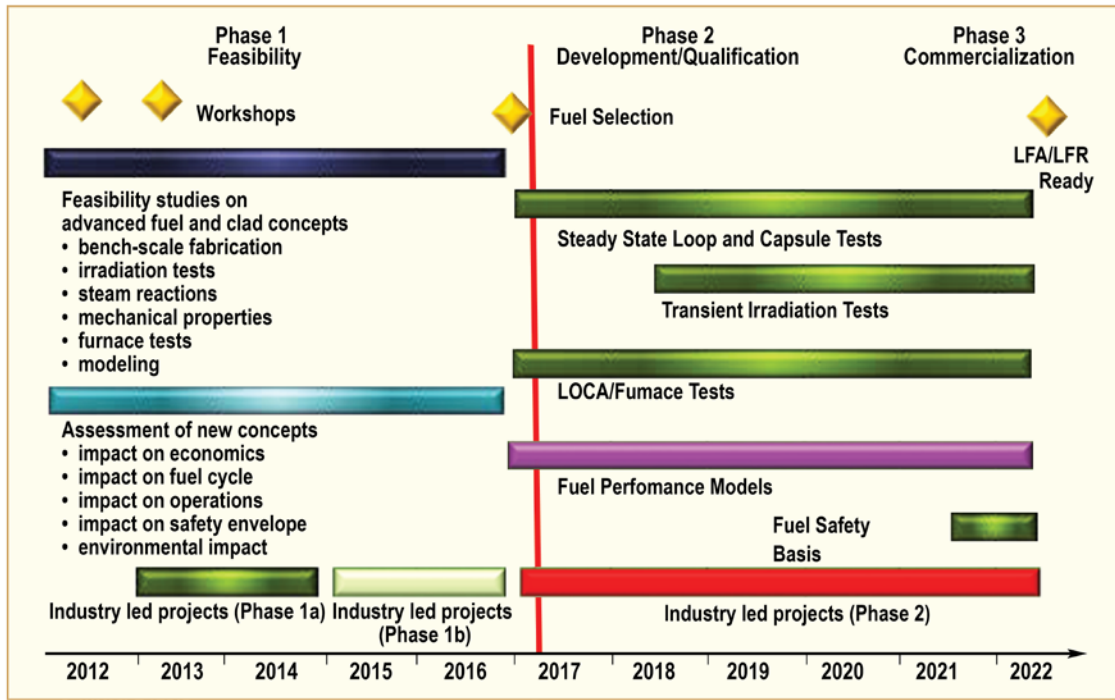
Figure 9-3:   US strategy for ATF R&D- development and qualification of ATF [McCaughey, 2017].

The ATF development effort adopts a three-phase approach to commercialization, as illustrated in Fig. 3. Each development phase roughly corresponds to the Technology Readiness Levels (TRL) defined for nuclear fuel development, where

- TRL 1-3 corresponds to the "proof-of-concept" stage,
- TRL 4-6 to "proof-of-principle," and
- TRL 7-9 to "proof-of-performance".

Each step in the fuel development effort necessarily considers the requirements set out by the Nuclear Regulatory Commission (NRC) to support the fuel licensing effort in planning, executing, and documenting all phases of fuel development, including fabrication, experiments, model development, and validation, etc.

9.2.1   National laboratory, Industry, and University directed efforts

Table 9-1 gives a summary of the major US DOE-funded ATF projects that are being led by a national laboratory, industry, or a university.

Table 9-1:   Major US DOE-funded ATF projects [Bragg-Sitton, 2015].

Lead Organization	Category-Major Technology Area	Additional Collaborators
Oak Ridge National Laboratory	Fuel: Fully Ceramic Microencapsulated (FCM)UO_2; FCM-UN	LANL, INL support FeCrAl weld development work
	Cladding: FeCrAl alloy; silicon carbide (SiC)	
Los Alamos National Lab	Fuel: Enhanced UO_2, Composite Fuels	
EPRI +LANL	Cladding: Advanced molybdenum alloys (multi-layer design)	ORNL
AREVA (FOA, NEUP)	Fuel: High Conductivity fuel ($UO_2+Cr_2O_3$ +SiC)	U. Wisconsin, U. Florida, SRNL, TVA, Duke
	Cladding: Coated Zr-alloys (protective materials, MAX phase)	
Westinghouse (FOA, NEUP)	Fuel: U_3Si_2, and UN+U_3Si_2 fuel	General Atomics, EWI, INL, LANL,MIT,TAMU, Southern Nuclear Operating Company
	Cladding: Coated Zr-alloy; SiC concepts	
GE Global Research (FOA)	Cladding: Advanced Steel (Ferritic/Martensitic, including FeCrAl)	Global Nuclear Fuels, LANL, U. Michigan
University of Illinois (IRP)	Cladding: Modified Zr-based cladding (coating or modification of bulk cladding composition)	U. Michigan, U. Florida, INL, U. Manchester, ATI Wah Chang **UK contributions
University of Tennessee (IRP)	Cladding: Ceramic Coatings for Cladding (MAX phase; multilayer ceramic coatings)	Penn State, U. Michigan, UC Boulder, LANL, Westinghouse, Oxford, U. Manchester, U. Sheffield, U. Huddersfield, ANSTO **UK and Australian contributions
Additional laboratories are providing analysis support (INL, BNL, ANL)		
		© ANT International 2017

The major fuel vendors, AREVA, GNF, and Westinghouse, are pursuing a wide range of promising eATF concepts under this DOE funded effort (Figure 9-4).This DOE program makes use of international collaborations as well, as shown in Figure 9-5 [McCaughey, 2017].

Figure 9-4:   Fuel vendor Teams are pursuing a Wide Range of Promising Concepts [McCaughey, 2017].
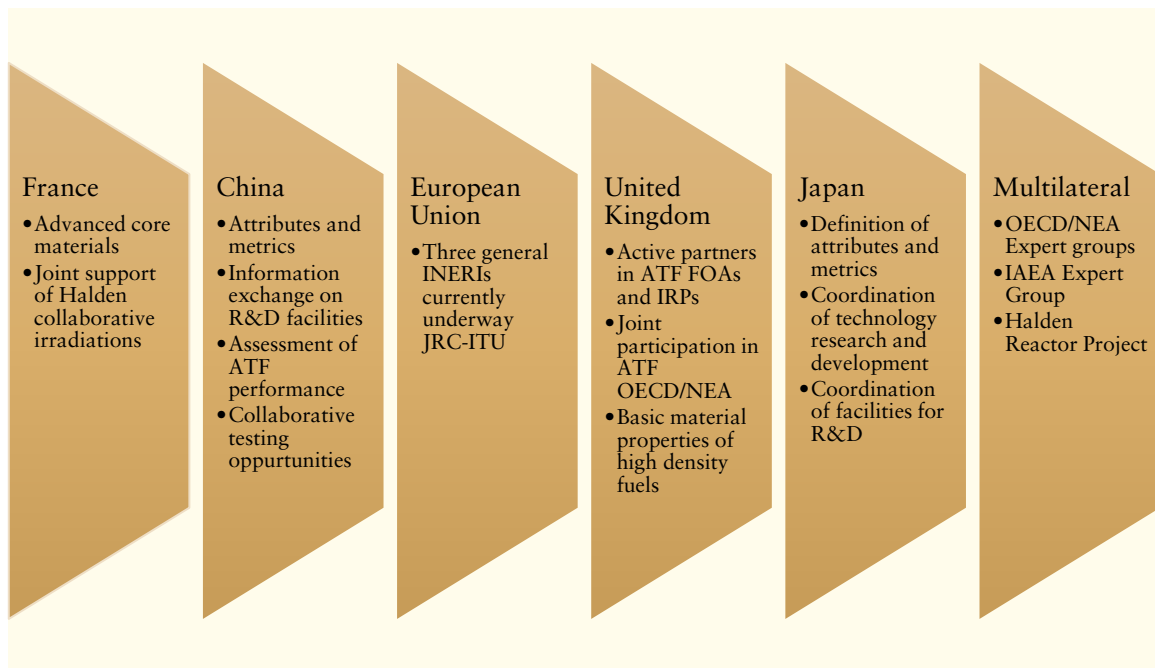

Figure 9-5:   International Collaborations Include Significant Development Partners [McCaughey, 2017].

9.2.2   ATF irradiation testing

An ATF irradiation test plan was developed for normal operating conditions to integral demonstrations under accident conditions to support the LTR/LTA program and finally qualification of an ATF concept. The test plan details are given in Table 9-2.

10 Storage and transportation of commercial spent nuclear fuel under dry, inert conditions (Albert Machiels)

10.1 Introduction

In last year's Annual Report Section 10 [Adamson R. et al., 2016], the impact of dry storage conditions on the behavior of hydrogen in zirconium-based alloys, which is picked up during in-reactor operation, was discussed with emphasis on (1) hydride dissolution and re-precipitation occurring during the thermal cycle inherent to dry storage, (2) environmental parameters (hydrogen concentration, temperature and stress gradients) governing hydrogen diffusion, (3) critical parameters governing hydride re-orientation from circumferential to radial, and (4) axial migration of hydrogen along the length of cladding tubes. Conclusions from the review were as follows:

- At the beginning of dry storage, maximum temperatures (up to 400°C) are high enough for hydrogen concentrations up to ~210 wppm (based on the TSSD of [Kammenzind et al., 1996] for unirradiated Zircaloy-4) to enter solid solution within the α-Zr matrix. However, only a very limited, if any, amount of the cladding material in a storage container would experience such high peak temperature. In alloys that contain hydrogen concentrations up to ~200-wppm, all hydrogen could be in solid solution at the locations where high peak temperatures are experienced. In alloys with concentrations greater than this value, the excess hydrogen will remain as hydride. Soluble hydrogen diffusion is driven by gradients in concentration, temperature, and stress. Insoluble hydride phases are immobile and act as sinks or sources for the precipitation or dissolution of hydrogen during temperature changes. When temperature decreases due to the falloff of decay heat with increasing storage time, hydrogen is expected to either re-precipitate close to previously existing ("memory" effect) and still existing hydrides (sympathetic "growth"), or form new hydrides ("nucleation").

- Temperatures are high enough during drying and early dry storage such that soluble hydrogen is expected to reach an equilibrium concentration at a given axial location by diffusion across the thickness of the SNF cladding wall. During cooling, hydrides may form preferentially in the Zr liner at the inner surface of BWR Zry-2 tubes or in the corrosion-resistant outer shell of PWR duplex claddings; both inner liner and outer shell are thermodynamically favoured over precipitation in the alloy matrix. Diffusion of soluble hydrogen to these regions decreases the concentration in adjacent regions and, in limiting cases, create zones that are essentially free of hydrides.

- Soluble hydrogen that precipitates on cooling in tensile stress fields greater than a threshold value, which varies with the alloy and its microstructure, can align themselves in a direction that is normal to the stress field, forming radially oriented hydrides. The extent of such reorientation and the effective continuity[11] of newly precipitated hydrides in the radial direction varies with material (texture, grain shape, hydrogen content), thermal cycling parameters (peak temperature, cooling rate, cladding stress state). Cladding ductility and impact resistance can be significantly degraded by a high degree of continuity of hydrides in the radial direction.

In this year's report, the degradation in ductility by hydrides is summarized given its potential relevance to accident analyses, especially for transportation of spent fuel after long storage times. High impact loads (transportation) and lower temperatures (long storage durations) are important

---

[11] A useful index appears to be the radial hydride continuity factor (RHCF). This index considers the effective length of interconnected or nearly-continuous hydrides that are aligned in the radial direction relative to the wall thickness, [Burtseva et al., 2010]. The continuity index is independent of the total hydrogen concentration and can take on large values even with small hydrogen concentrations.

conditions when assessing the performance of spent LWR fuel assemblies under hypothetical accident conditions. A summary of several papers presented at the 2017 Water Reactor Fuel Performance Meeting held on September 10 - 14 in Jeju, Jeju Island, Korea will also be presented.

10.2 Transportation of spent nuclear fuel

10.2.1 Licensing considerations

When dealing with transportation of high burnup fuel, defined as fuel assemblies with assembly-averaged burnup > 45 GWd/MTU), most of the regulatory interactions (and R&D) have been centred on two key regulatory requirements [NRC, 1984], which can be summarized as follows:

- The geometric form of the package contents should not be substantially altered under normal conditions of transport; and

- Sub-criticality must be maintained under all normal and accident transport conditions.

Maintaining cladding and fuel assembly integrity under hypothetical accident conditions helps greatly in satisfying the sub-criticality regulations that require that the transportation package contents remain subcritical when assuming water intrusion.

- For burnups less than or equal to 45 GWd/MTU, the US NRC has accepted that hypothetical transportation accidents do not result in significant damage to, or reconfiguration of the spent fuel. Therefore, spent fuel is assumed to remain structurally intact under hypothetical accident conditions, and its nuclear reactivity remains bounded by the criticality analysis performed to demonstrate compliance for the "as-loaded" or "as-designed" configuration.

- For burnups greater than 45 GWd/MTU, the NRC concluded that they could not rule out significant fuel damage and fuel reconfiguration.[12] Therefore, the sub-criticality requirement may have to be addressed, unless it can be demonstrated that intrusion of water can be ruled out (i.e., "moderator exclusion") [EPRI, 2005].

Studies sponsored by the Electric Power Research Institute (EPRI), the US Department of Energy (DOE), and the US Nuclear Regulatory Commission (NRC) have shown that fuel reconfiguration resulting in sufficient nuclear reactivity to create a criticality event is not credible. The effects on spent fuel's nuclear reactivity from "worst-case" accident scenarios were surveyed in NUREG/CR-6835 [Elam, 2002], ORNL/TM-2012/325 [Marshall and Wagner, 2012], and NUREG-CR-7203 [Scaglione et al., 2015]. These surveys used scenarios that were postulated to provide theoretical upper limits for reactivity effects of fuel relocation, although some were described as going "beyond credible conditions." These scenarios involved physical changes either to fuel assembly rod arrays or to collections of fuel pellets with the fuel skeleton removed. Given that many of the chosen scenarios were not physically possible, EPRI sponsored a methodology that (1) deconstructed each scenario in NUREG/CR-6835 into a set of sub-scenarios and (2) identified the physical phenomena required to create the sub-scenario to provide more credible estimates of the probability and associated maximum changes in nuclear reactivity [EPRI, 2007; Wells and Machiels, 2012]. The boundary between credible, but unlikely, scenarios and incredible scenarios was more easily discernible with this process.

- Rod array scenarios, which essentially consider changing the fuel rod pitch (or spacing between fuel rods) in the limited space of a basket cell, were evaluated and the guidance in

---

[12] "*It is judged that, at this time, there is insufficient material property information for high burnup fuel to allow this type of evaluation.*" Excerpt from Interim Staff Guidance 19, *Moderator Exclusion under Hypothetical Accident Conditions and Demonstrating Subcriticality of Spent Fuel under the Requirements of 10 CFR 71.55(e)*, NRC Spent Fuel Project Office (May 2003)

ANSI/ANS-8.1 related to the double-contingency principle[13] was followed. Such scenarios assume failure of structural assembly components such as grids and spacers, but fuel rod geometry is assumed to be maintained. The results show a maximum reactivity increase in the neutron multiplication factor, k_{eff}, of ~0.03, which is less than the administrative margin of 0.05, meaning sub-criticality is maintained.[14]

- Fuel pellet array scenarios, which essentially consider the fuel to be reduced to the form of debris, were also evaluated; the evaluation shows that the establishment of an optimally moderated lattice of fuel pellets is not credible. The more likely outcome is under-moderated debris heaps resulting in large reactivity decreases.

When considering transportation accidents, and more specifically extensive longitudinal (axial) tearing damage to fuel rods caused by massive hydride re-orientation, the more likely scenarios would be fuel pellet array scenarios resulting in large nuclear reactivity decreases. From these studies, it can be concluded that the requirement for ensuring sub-criticality under hypothetical accident conditions will be satisfied, even assuming extreme damage to the spent high-burnup fuel rods [EPRI, 2010]. In addition, transportation risk assessments sponsored by NRC [NRC, 2014; Meiner and Ammerman, 2014; EPRI, 2008] show that the combination of factors necessary to produce an accident that leads to a criticality event is so unlikely that the event should be considered as not credible.

For normal conditions of transport, large margins against fuel rod failures are predicted. Grids and guide tubes, which form the structural elements of the fuel assembly, are also predicted to remain structurally competent. Table III-10 in Sandia report SAND90-2406 [Sanders T.L. et al., 1982] shows that, under normal conditions of transport for low burnup fuel, pinch loading forces acting on fuel rod cladding in a PWR B&W 15x15 design are calculated to be 79.2 N at the spacer grid support due to shock and vibration loadings; this results in a rod breakage probability of $2x10^{-12}$, which is negligible. However, the evaluation of each package design under normal conditions of transport must include a determination of the effect of a free 0.3-m drop test onto a flat, essentially unyielding, horizontal surface, striking the surface in a position for which maximum damage is expected. For such a scenario, the pin loading forces are calculated to be ~50 times greater than those generated by shock and vibration loadings. In addition, for high-burnup fuel, rod breakage probabilities need to be modified to include the potential impact of radial hydrides. As a result, a more thorough assessment was performed and documented in EPRI report 1015049 [EPRI, 2007]. The calculated rod breakage probability was calculated to be equal to $2x10^{-8}$, which is also very small.[15]

10.3 Ductility degradation by hydrides

10.3.1 Ductility reduction by hydrides

Zirconium hydrides are brittle and can negatively affect the ductility of zirconium-based alloys. Ductility is observed to depend on hydride distribution, density, orientation, and temperature. For information, hydride-assisted degradation of ductility and fracture toughness of Zr-alloys is described

---

[13] The "double contingency principle," as used in ANSI/ANS-8.1-1983*, states that process designs should, in general, incorporate sufficient factors of safety to require at least two unlikely, independent, and concurrent changes in process conditions before a criticality accident is possible.".

[14] To provide additional confidence that no criticality occurs, NRC limits the maximum neutron multiplication factor, k_{eff}, to 0.95. A critical configuration requires at a minimum $k_{eff} = 1$. In addition, NRC requires that criticality calculations be performed in such a way that uncertainties in the values of the parameters in the calculation are accounted for by using the "worst" value of the parameter range (leading to the highest k_{eff} value). In addition, corrections include non-conservative biases in analytical models that do not conservatively fit criticality benchmark data to protect against underestimation of k_{eff}.

[15] Given there are approximately 10^4 fuel rods in a typical, large transportation cask, this means the probability of just one rod breaking under the 0.3-meter side drop accident scenario would be on the order of 10^{-4}.

in detail in the ZIRAT13/IZNA8 Special Topic Reports on hydrogen, [Strasser et al., 2008a] and [Strasser et al., 2008b].

The effect of hydrides is strongly dependent on testing temperature. At temperatures above 300°C (reactor operating regime and higher temperature range of realistic storage and transportation conditions), ductility is controlled by irradiation damage and is relatively insensitive to uniformly distributed hydrogen contents below about 1000 wppm, as shown in Figure 10-1 (data obtained on Zircaloy-4 fuel cladding). At temperatures near room temperature, ductility is significantly reduced by hydrogen content, as illustrated in Figure 10-2 (data obtained on Zircaloy-4 guide tube); the effects of irradiation and hydrides appear to be additive.

The effect of hydrides is also strongly dependent on the orientation of the hydrides, as visualized by the orientation of the stacking of the hydride platelets, relative to the applied stress. This is illustrated in Figures 10-3 and 10-4 obtained on Zircaloy-4 cladding specimens containing increasing amounts of radial hydrides. The effect was assessed using uniaxial tensile testing, for which the applied stress is parallel to the radial hydrides, and slotted-arc tension tests for which the applied stress is perpendicular to the radial hydrides. Both tests were conducted at room temperature and at 300°C. As can be seen, the effect of radial hydrides on total and uniform elongations is negligible at both room temperature (Figure 10-16 (a)) and 300°C (Figure 10-16 (b)) when applied stress and radial hydride orientation are parallel to each other. However, this is no longer the case, at least at room temperature, when applied stress and radial hydride orientation are perpendicular to each other (Figure 10-4a); at 300°C, however, radial hydrides have no effect (Figure 10-4b), consistent with the trend shown in Figure 10-1. Analysis with scanning electron metallography indicated that the observed decrease in ductility at room temperature correlated with the "effective hydride spacing".
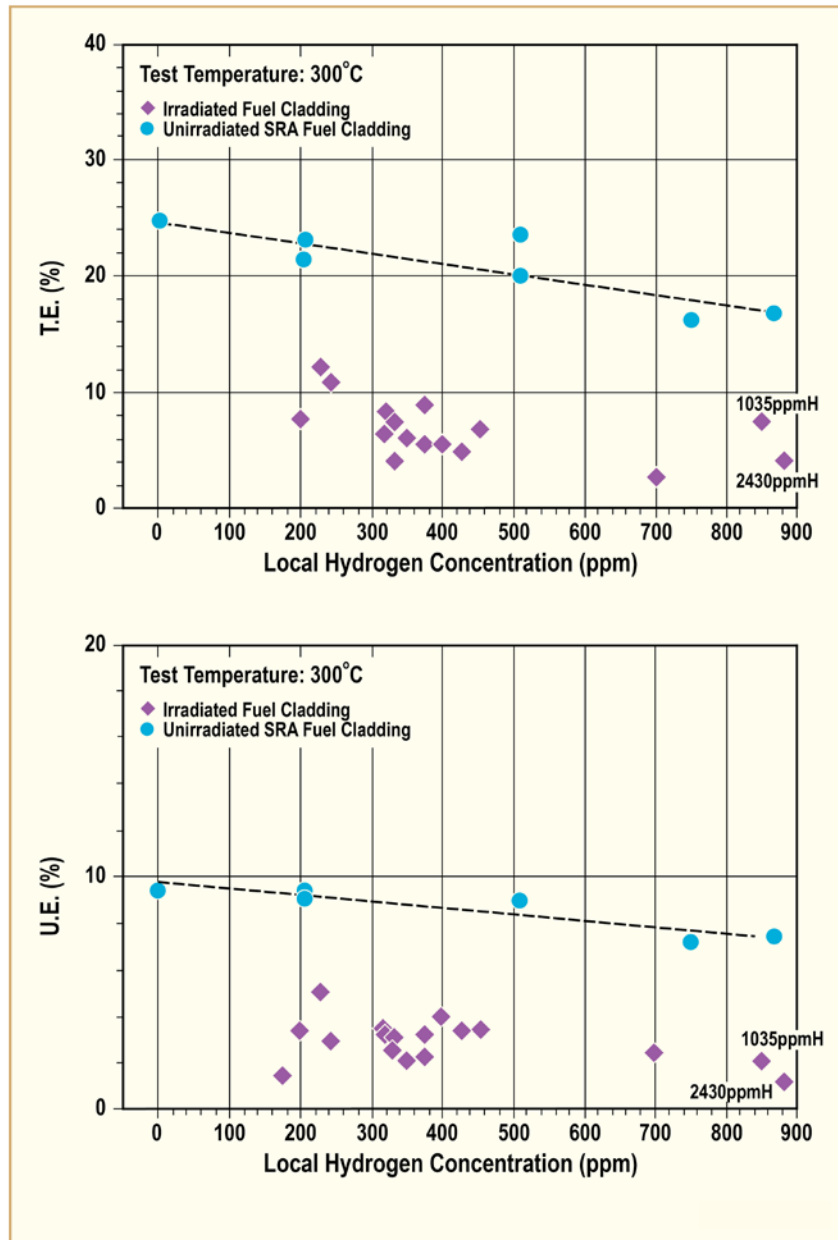
Figure 10-1:   Total and Uniform Elongation for unirradiated and irradiated Zircaloy-4 cladding specimens as a function of hydrogen concentration; data obtained by uniaxial testing at 300°C with uniformly distributed hydrides in a predominantly circumferential orientation [Yagnik et al., 2004]
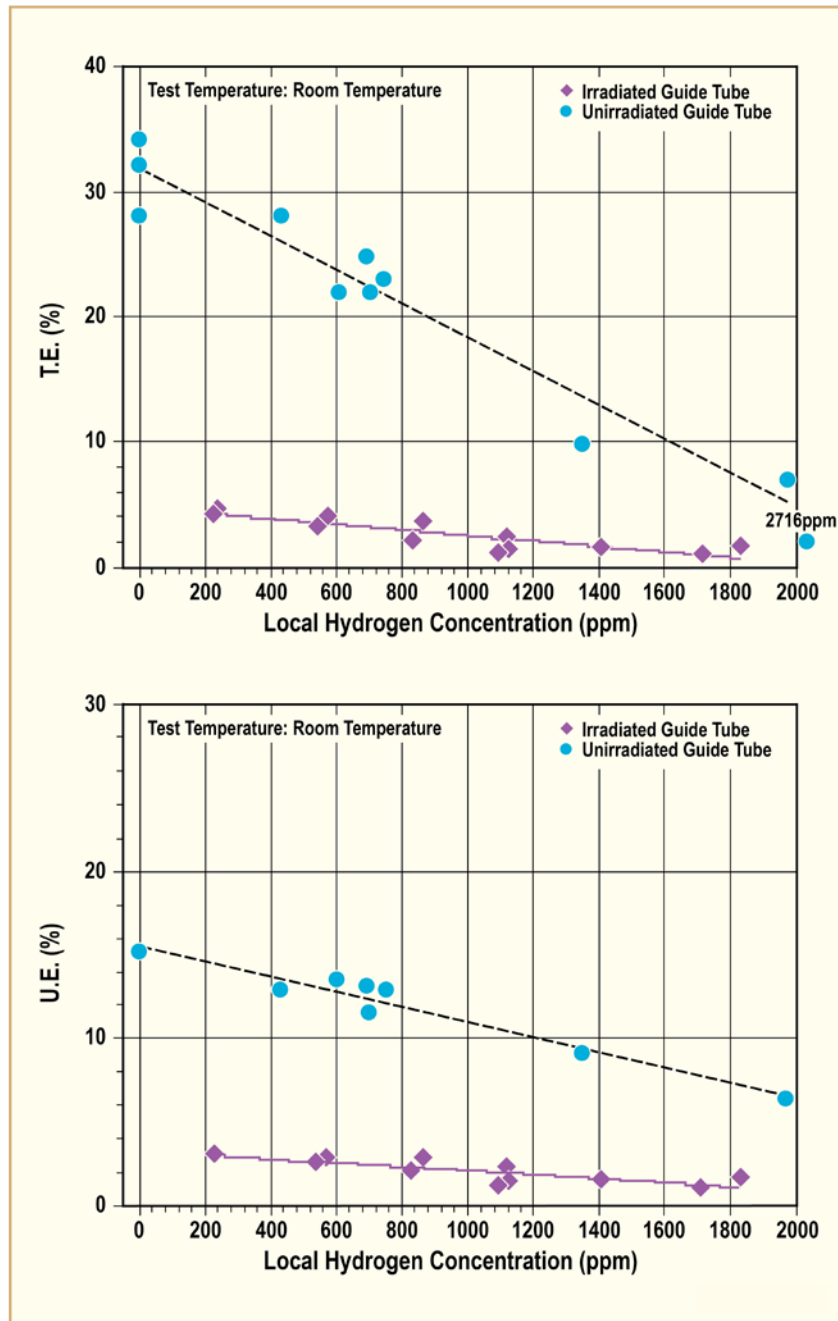
Figure 10-2:   Total and Uniform Elongation for unirradiated and irradiated Zircaloy-4 guide tube specimens as a function of hydrogen concentration; data obtained by uniaxial testing at room temperature with uniformly distributed hydrides in a predominantly circumferential orientation [Yagnik et al., 2004.]

11 Trends and needs

Improved fuel reliability and operating economics are the driving forces for changing operating conditions, while at the same time maintaining acceptable margins to operating and regulatory safety limits. Table 11-1 gives the trends for Burn Up (BU) achieved compared to regulatory limits in various countries. An approximate ("rule of thumb") conversion of BU to fluence is 50 GWd/MT is equivalent to about 1×10^{22} n/cm^2, E>1 MeV (or about 17 dpa), but this depends on many nuclear parameters such as enrichment, extent of moderation and neutron energy spectrum. In general, PWRs operate to higher discharge BUs compared to BWR because of higher PWR power densities and neutron fluxes, but the differences are decreasing with time. There are some incentives to reach BUs of 60-70 GWd/MT batch average, but the economic values of doing so are decreasing. A majority of US plants and many in Europe have undergone power uprates, from a few percent to up to 20%. This increases the number of Fuel Assemblies (FAs) in a core that operates at high power, thereby decreasing the margin to established limits. In cooperation with utilities, fuel suppliers have operated LTA or LUAs to very high BUs, in some cases approaching 100 GWd/MT peak rod exposures.

Table 11-1: Maximum BUs achieved vs. regulatory limits, (excludes LTAs).

Country	BU (GWD/MT)				Regulatory Limit
	Batch	Assembly	Rod	Pellet	
USA	57	60	62	73	62.5 peak rod
Belgium		50-55			55 UO$_2$ assy., 50 MOX assy.
Czech Republic	51	56	61		60 peak rod
Finland	45.6*	48.6	58		57 assy. (for PWR)
France	47	51 UO$_2$ 42 MOX			52 assy.
Germany	58	62	68		65 assy.
Hungary		50	62		
Japan	53	55	62		55 UO$_2$ assy., 45 MOX assy.
Korean Republic	46				60 rod
Netherlands	52	55	59		60 rod
Russia	60	65			
Spain	50.4	57.4	61.7	69	
Sweden	47	57.2	63.6	65	60 assy., 64 rod
Switzerland	68	71	73		80 pellet
Taiwan					60 rod (P), 54 assy. (B)
UK	44.3	46.5	50		55 pellet
Ukraine		50			
*Current batch design for 50 GWD/MT in BWR					
					ANT International, 2014

As discussed in earlier sections, material properties and microstructure evolve as BU and fluence become higher. Examples include:

In PWRs, Zry-4 no longer meets corrosion and hydriding performance needs; therefore, virtually all current PWR claddings now use a zirconium alloy containing Nb.

Although not a new phenomenon, observed Second Phase Particle (SPP) dissolution and re-precipitation phenomena have required a new perspective on alloy development and Hydrogen Pick Up (HPU).

BWR channels' bow at high BU has required a new understanding of the relationships between HPU, shadow corrosion and irradiation growth.

A broader listing of issues needing resolution include:

Corrosion related to oxide thickness and H pickup:

- BWRs and PWRs:
    o Effects of solid and high concentration of hydrides on corrosion mechanism.
    o Effect of Nb.
    o Mechanism of HPU, including diffusion of species to the metal-oxide interface, ; role of SPP dissolution; role of internal space charges
    o Integration of atomistic modelling, high resolution "microscopy" and mechanistic "theory" modeling
    o Role of <c.-component loops on hardness and strength
- BWRs:
    o Shadow corrosion mechanisms and its relation to channel bow.
    o Late increased corrosion and HPU of Zry-2 at high BU's burnups– with and without shadow corrosion
    o Kinetics of hydriding in the shadow corrosion-affected channel surfaces
    o Localised hydriding – Browns Ferry – new failure mechanism
    o CRUD-chemistry-corrosion interactions.
    o Effect of water chemistry impurities, as well as specific effects of NMCA, with or without Zn-injection.
- PWRs:
    o Effects of surface contaminations and/or boiling on Zr-Nb alloys.
    o Welding of the new alloys may need improved processes (Zr-Nb alloys).
    o Effect of increased Li together with increased duty (sub-cooled boiling) with and without Zn-injection.
    o Effects of increased hydrogen coolant content (to mitigate Primary Water Stress Corrosion Cracking (PWSCC)).
    o Axial offset anomaly (AOA) mechanisms.
    o Mechanism of improved corrosion due to Nb additions

Mechanical properties related to irradiation and H pickup:

- Decreased ductility and fracture toughness as consequences of the increased HPU and formation of radial hydrides during any situation (e.g., RIA, PCMI, LOCA and post-LOCA events, seismic event, transport container drop-accident conditions).
- Quantification of the effect of irradiation on the apparent solubility of hydrogen, and mechanism by which the phenomenon occurs.
- Details of deformation mechanisms in zirconium alloys, including being able to predict the dislocation channelling system.
- Development of micromechanical models applicable to deformation at appropriate component conditions.

References

ABAQUS/Standard, *ABAQUS Explicit, Version 5.8*, ABAQUS Inc., Providence, USA, 1998.

Abe, H. et al, *Development of advanced expansion due to compression (A-EDC) test method for safety evaluation of degraded nuclear fuel cladding materials*, Journal of Nuclear Science and Technology, 52, pp. 1232–1239, 2015.

Adamson R. et al., *In-Reactor Creep of Zirconium Alloys*, ZIRAT14/IZNA9 Special Topical Report, ANT International, Mölnlycke, Sweden, 2009.

Adamson R. et al., *Annual Report*, ZIRAT16, ANT International, Mölnlycke, Sweden, 2011.

Adamson R et al., *Annual Report*, ZIRAT21/IZNA16, ANT International, Mölnlycke, Sweden, 2016.

Adamson R. et al., C., *Irradiation Growth – A Review*, ZIRAT 22 Special Topical Report, ANT International, Mölnlycke, Sweden, 2017.

Aitchison I., and Davies P.H., *Role of microsegregation in fracture of cold-worked Zr-2.5Nb pressure tubes,* Journal of Nuclear Materials, 203, pp. 206-220, 1993.

Anonymous, *Standard test methods for tension testing of metallic materials,* ASTM International, E8/E8M-16a, 2016.

Baek J-K et al., *The Oxidation Behavior Of The Silicide/Aluminide Coated Molybdenum And Niobium Specimens*, 2017 Water Reactor Fuel Performance Meeting, Jeju Island, South Korea, Sep. 10-14, 2017

Barrett K. et al., *Advanced LWR Nuclear Fuel Cladding System Development Trade-off Study*, INL/EXT-12-27090, September 2012

Barrow, A.T.W.,Korinek, A., and Daymond, M.R., *Evaluating zirconium-zirconiumhydride interfacial strains by nano-beam electron diffraction*, Journal of Nuclear Materials,432,pp. 366-370, 2013.

Beale, J., *Fuel Performance Data*, International Utility Nuclear Fuel Performance Conference, June 22-23, 2016, Charlotte, North Carolina, USA, 2016.

Besmann, T. et al., *Modeling Thermochemistry of Fuel and Coupling to Fuel Performance Codes*, Top Fuel 2016, Boise, Idaho, USA, American Nuclear Society, 2016

Bischoff J. et al., *Development of Cr-coated Zirconium Alloy Cladding for Enhanced Accident Tolerance*, Top Fuel 2016, Boise, ID, September 11-15, 2016

Bischoff J., *Development of Cr-coated Zirconium Alloy Cladding for Enhanced Accident Tolerance*, proceedings ofTop Fuel 2016, Boise, Idaho, USA, Sept. 11-16, 2016

Bischoff J. et al., *AREVA NP's Enhanced Accident Tolerant Fuel Developments: Focus On Cr coated M5™ Cladding*, 2017 Water Reactor Fuel Performance Meeting, Jeju Island, South Korea, Sep. 10-14, 2017

Björk K. I. et al., *Test Irradiation Of Enhanced Nuclear Fuel And Cladding*, 2017 Water Reactor Fuel Performance Meeting, Jeju Island, South Korea, Sep. 10-14, 2017

Blackmur, M.S. et al., *Zirconium hydride precipitation kinetics in Zircaloy-4 observed with synchrotron x-ray diffraction,* Journal of Nuclear Materials, 464, pp. 160-169, 2015.

Boado Magan, H., F. et al., *CAREM project status*, Science and Technology of Nuclear Installations, 2011.

Bouffioux, P., Rupa, N., *Impact of Hydrogen on Plasticity and Creep of Unirradiated Zircaloy-4 Cladding Tubes*, ASTM Special Technical Publication 1354, pp. 399-422 2000

Brachet, J. C. et al., *Behavior under LOCA conditions of Enhanced Accident Tolerant Chromium Coated Zircaloy-4 Claddings*, Top Fuel 2016, Boise, ID, September 11-15, 2016

Brachet J. C. et al., *Behavior Of Chromium Coated M5TM Claddings Under LOCA Conditions*, 2017 Water Reactor Fuel Performance Meeting, Jeju Island, South Korea, Sep. 10-14, 2017

Bragg-Sitton, S., *Development of advanced accident-tolerant fuels for commercial LWRs,* Nuclear News, 57, pp. 83-91, 2014.

Bragg-Sitton S., *Update on Accident Tolerant Fuel and IAEA Technical Meeting on ATF*, April 2015

Bragg-Sitton et al., *Evaluation of Enhanced Accident Tolerant LWR Fuels*, Top Fuel, 2015.

Bragg-Sitton S., *Overview of the U.S. Department of Energy Program on the Development of Enhanced Accident Tolerant Fuels for LWRs*, 2016 Accident Tolerant Fuel (ATF) workshop on System Assessment and Materials, Shenzhen, June 23–24, 2016

Bragg-Sitton S. and Carmack W. J., *Phased Development of Accident Tolerant Fuel*, Top Fuel 2016, Boise, ID, September 11-15, 2016

Cantonwine, P. et al., *GNF Fuel Performance 2015 Update*, TopFuel 2015: Light Water Reactor Fuel Performance Meeting, Zurich, Switzerland, European Nuclear Society, pp 295-304, 2015.

Cantonwine, et al., *The Performance of NSF in BWR Operating Conditions*, Zirconium in the Nuclear Industry: 18th International Symposium, ASTM STP1597, R. J. Comstock and A. T. Motta, Eds., ASTM International, West Conshohocken, PA, 2017 in press.

Chapin D. et al., *Design and Operation of EFG Fuel in Ringhals PWRs*, TopFuel 2013, Charlotte, NC, September, 2013.

Cheng B. et al., *Fabrication of Rodlets with Coated and Lined Mo-alloy Cladding for Testing and Irradiation*, Top Fuel, Boise, ID, September 2016

Cheng B. et al., *Zr-Alloy Lined Molybdenum Fuel Cladding To Enhanced Accident Tolerance*, 2017 Water Reactor Fuel Performance Meeting, Jeju Island, South Korea, Sep. 10-14, 2017

Christensen M. et al., *Diffusion of point defects, nucleation of dislocation loops, and effects of hydrogen in hcp-Zr: Ab initio and classical simulations,* Journal of Nuclear Materials, 460, pp. 82-96, 2015.

CNNC, ACP100 *Technical & Economic Aspects*, Technical Meeting on Economic Analysis for HTGR and SMR, Vienna, Austria, 2015.

Colas K.B et al., *Effect of thermo-mechanical cycling on zirconium hydride reorientation studied in situ with synchrotron X-ray diffraction*, Journal of Nuclear Materials, 440, pp. 586-595, 2013.

Coleman. C.E., Theaker, J.R., Kidd, K.V., *Effect of fabrication variables on irradiation response of crack growth resistance of Zr-2.5Nb,* Zirconium in the Nuclear Industry: Fourteenth International Symposium, ASTM STP 1467, pp. 783-801, 2006.

Cottrell A., *Dislocation Theory of Yielding and Strain Ageing of Iron*, Proceedings of the Physical Society, Section A, Volume 62, Issue 1, pp. 49-62, 1949

Crank J., *The mathematics of Diffusion*, 2nd ed., Oxford University Press, pp. 32-47, 1975.

Daub K. et al., *Investigating potential accident tolerant fuel cladding materials and coatings*, 18th International Conference on Environmental Degradation of Materials in Nuclear Power Systems – Water Reactors, Portland, OR., August 2017.

Daum R.S et al., *Identification and quantification of hydride phases in Zircaloy-4 cladding using synchrotron x-ray diffraction*, Journal of Nuclear Materials, 392, pp. 453-463, 2009.

List of common abbreviations

appm	Atomic Parts Per Million		DZO	Depleted Zinc Oxide
ADS	Automatic Depressurization System		EB	Electron Beam
			EBR	Experimental Breeder Reactor
AE	Acoustic Emission		EBSD	Electron Backscatter Diffraction
ANL	Argonne National Laboratory		ECCS	Emergency Core Cooling System
ANT	Advanced Nuclear Technology		ECR	Equivalent Cladding Reacted
AOA	Axial Offset Anomaly		EDC	Expansion Due to Compression
AOO	Anticipated Operational Occurrences		EdF	Electricité de France
			EDS	Energy Dispersive Spectroscopy
APT	Atom Probe Tomography		EDX	Energy Dispersive X-ray spectroscopy
AR	Annual Report			
AREVA	French Equipment Manufacturer		EELS	Electron Energy Loss Spectroscopy
ASTM	American Society for Testing and Materials			
			EFPD	Effective Full Power Days
AT	Axial Tensile		EOL	End Of Life
ATEM	Analytical Transmission Electron Microscope		EPMA	Electron Probe Micro-Analysis
			EPRI	Electric Power Research Institute
ATP	Atom Probe Tomography		ESCP	Extended Storage Collaboration Program
ATR	Advanced Test Reactor			
B&W	Babcock & Wilcox		ESSC	Enhanced Spacer Shadow Corrosion
BCC	Body Centered Cubic			
BDB	Beyond Design Basis		ETR	Engineering Test Reactor
BE	Back End		FA	Fuel Assembly
BN	Belgo-Nucleare		FBR	Fast Breeder Reactor
BNL	Brookhaven National Laboratory		FC	Fuel Channel
BOL	Beginning of Life		FCC	Face Centered Cubic
BU	Burn-Up		FCI	Fuel Cladding Interaction
BWR	Boiling Water Reactor		FCM	Fully Ceramic Micro-Encapsulated
CANDU	Canadian Deuterium Uranium			
CB	Channel Bow		FCT	Fuel Centreline Temperature
CCT	"C"-shaped ring Compression test		FE	Front End
CEA	Commissariat à l'Energie Atomique		FFRD	Fuel Fragmentation, Relocation, and Dispersal
			FGR	Fission Gas Release
CILC	CRUD Induced Localised Corrosion		FIB	Field Ion Bombardment
			FIB	Focused Ion Beam
CIM	Channel Interference Metric		FIMA	Fissions per Initial Metal Atom
CPR	Critical Power Ratio		FR	Fuel Rod
CRP	Coordinated Research Project		FWHM	Full Width Half Maximum
CRUD	Chalk River Unidentified Deposits		GB	Grain Boundary
CT	Central Tube		GDC	General Design Criteria
CT	Compact Tension		GE	General Electric
CVD	Chemical Vapour Deposition		GNF	Global Nuclear Fuel
CW	Cold Work		GT	Guide Tube
CWSR	Cold Work and Stress Relieved		GTRF	Grid-to-Rod Fretting
CZP	Cold Zero Power		HAADF	High Angle Annular Dark Field
DB	Deep Bed		HANA	High performance Alloy for Nuclear Application
DBA	Design Base Accident			
DCF	Dual Cooled Fuel		HB	High Burnup
DCP	Distinctive CRUD Pattern		HBS	High Burnup Structure
DFT	Density Functional Theory		HBWR	Halden BWR
DHC	Delayed Hydride Cracking		HDS	Hold-Down Spring
DNB	Post-Departure from Nucleate Boiling		HFIR	High Flux Irradiation Reactor
			HGCIM	Half-Gap Channel Interference Metric
DNBR	Departure from Nucleate Boiling Ratio			
			HIP	Hot Isostatic Pressing
DOE	Department of Energy		HPCI	High-Pressure Coolant Injections
DS	Dimensional Stability			

Unit conversion

TEMPERATURE		
°C + 273.15 = K	°C × 1.8 + 32 = °F	
T(K)	T(°C)	T(°F)
273	**0**	32
289	16	61
298	25	77
373	**100**	212
473	**200**	392
573	**300**	572
633	360	680
673	**400**	752
773	**500**	932
783	510	950
793	520	968
823	550	1022
833	560	1040
873	**600**	1112
878	605	1121
893	620	1148
923	650	1202
973	**700**	1292
1023	750	1382
1053	780	1436
1073	**800**	1472
1136	863	1585
1143	870	1598
1173	**900**	1652
1273	**1000**	1832
1343	1070	1958
1478	1204	**2200**

MASS	
kg	lbs
0.454	**1**
1	2.20

DISTANCE	
x (µm)	x (mils)
0.6	0.02
1	0.04
5	0.20
10	0.39
20	0.79
25	0.98
25.4	**1.00**
100	3.94

PRESSURE		
bar	MPa	psi
1	0.1	14
10	**1**	142
70	7	995
70.4	7.04	**1000**
100	10	1421
130	13	1847
155	15.5	2203
704	70.4	**10000**
1000	100	14211

STRESS INTENSITY FACTOR	
MPa√m	ksi√inch
0.91	**1**
1	1.10

Radioactivity
1 Sv = 100 Rem
1 Ci = 3.7×10^{10} Bq = 37 GBq
1 Bq = $1\ s^{-1}$